



## **Minitowers benches mechanical design and tests with a dummy bench**

**N. Allemandou, L. Giacobone, R. Gouaty, L. Journet, B. Lieunard, F. Marion,  
A. Masserot, B. Mours, E. Pacaud, A. Paixao, L. Rolland**



**VIR-0229A-14  
May 12<sup>th</sup>, 2014**

# Summary

<b>1</b>	<b>INTRODUCTION .....</b>	<b>3</b>
<b>2</b>	<b>WEIGHT OF THE EQUIPMENT PUT ON THE BENCHES .....</b>	<b>5</b>
<b>3</b>	<b>VERTICAL TUNING OF THE BENCH .....</b>	<b>6</b>
<b>4</b>	<b>THERMAL EFFECTS MODELING .....</b>	<b>8</b>
4.1	BENCH GEOMETRY .....	8
4.2	EMISSIVITY .....	8
4.2.1	<i>Emissivity of aluminium .....</i>	<i>8</i>
4.2.2	<i>Emissivity of stainless steel.....</i>	<i>9</i>
4.2.3	<i>Procedure to measure the emissivity .....</i>	<i>9</i>
4.3	BENCH THERMAL RADIATION MODEL.....	10
4.3.1	<i>Simple bench geometry.....</i>	<i>10</i>
4.3.2	<i>Effective emissivity.....</i>	<i>10</i>
4.3.3	<i>Bench temperature .....</i>	<i>11</i>
4.4	ESTIMATION OF THE TEMPERATURE GRADIENT INSIDE THE BENCH.....	11
4.4.1	<i>Temperature of the walls of the air tank.....</i>	<i>12</i>
4.4.2	<i>Thermal gradient inside the air tank shell or minitower shell:.....</i>	<i>12</i>
<b>5</b>	<b>HEAT TRANSFER TEST .....</b>	<b>13</b>
5.1	DUMMY BENCH USED FOR THIS TEST .....	13
5.2	INSTALLING THE DUMMY BENCH IN THE MINITOWER .....	14
5.3	POWER DISSIPATED IN THE DUMMY BENCH .....	14
5.4	TEST BEFORE MINITOWER SAND BLASTING .....	15
5.4.1	<i>Observed temperatures.....</i>	<i>15</i>
5.4.2	<i>Expected temperature difference .....</i>	<i>16</i>
5.4.3	<i>Temperature gradient inside the dummy bench.....</i>	<i>17</i>
5.5	TEST WITH SAND BLASTED MINITOWER.....	17
5.5.1	<i>Observed temperatures.....</i>	<i>17</i>
5.6	IMPACT OF ANODIZING AND SAND BLASTING ON THE VACUUM QUALITY .....	19
5.6.1	<i>Minitower pressure.....</i>	<i>19</i>
5.6.2	<i>Quality of the vacuum: RGA spectrums.....</i>	<i>21</i>
<b>6</b>	<b>FINITE ELEMENT MODELING.....</b>	<b>23</b>
6.1	GEOMETRY OF THE BENCH USED.....	23
6.2	STRESS OF THE ELECTRONIC AIR TANK WALLS .....	24
6.3	BENCH DEFORMATION DUE TO ITS WEIGHT .....	24
6.4	NORMAL MODES .....	25
6.4.1	<i>Mode 1 to 6: global motion of the bench .....</i>	<i>25</i>
6.4.2	<i>Mode 7 to 12: motions of the wire .....</i>	<i>26</i>
6.4.3	<i>First internal mode of the bench: 193 Hz.....</i>	<i>26</i>
6.4.4	<i>Next 3 modes: 204 to 210Hz.....</i>	<i>27</i>
<b>7</b>	<b>ANNEX: BENCH DRAWINGS USED FOR THE CALL FOR TENDER.....</b>	<b>28</b>

# 1 Introduction

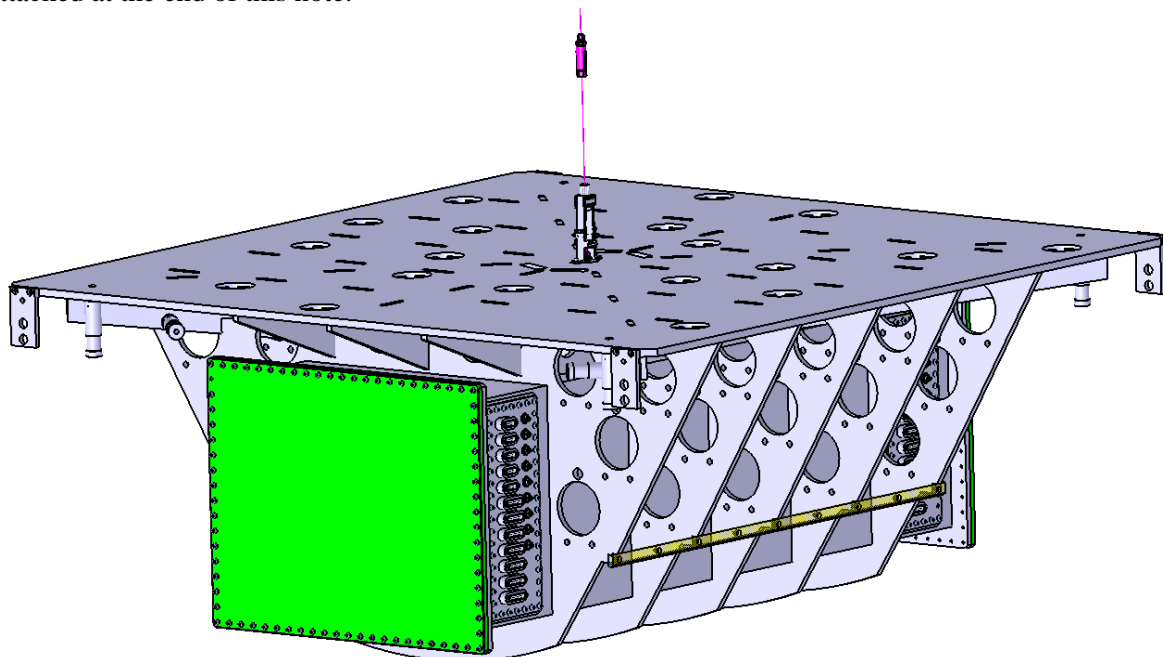
This note describes the mechanical design of the minitower benches and the validations studies made during the design phase.

It assumes the optical layout of VIR-0433A-13 and cabling described in VIR-0458A-13.

The benches have been designed with the following parts and guidelines:

- A top surface with a grid of M6 holes every 25mm like on any usual optical table. This grid is centered on the bench center. This surface is equipped with holes for the cabling of the various equipments (photodiodes and so one) which are closed when not in use.
- A M12 threaded hole at its center to attach the support steel wire which does the connection to the minitower seismic isolation system developed at Nikhef: mSAS. This bending point of the wire should be close enough to the center of mass to provide low frequency tilt modes.
- Ribs to make the bench stiff enough to have its first internal modes above about 150Hz which correspond to a little more of the main vertical mode of mSAS.
- An air tight box to host the electronic modules in the bottom part of the bench. Its purpose is to limit the number of cables running along mSAS to keep the good seismic isolation performances. This air tight box must be equipped with feedthroughs for the various cables and removable doors at its end to access the electronic.
- The electronic will use a few hundred watts of power. This power could only be dissipated through radiation, since the bench is under vacuum and connected to the ground by the single suspension wire and mSAS. Therefore the bench must have a good emissivity and should be made of a material with good thermal conductivity to use the entire bench surface as radiator. Anodized aluminum has been selected and tests are described in this note.
- Due to the required fine tuning of mSAS, the total weight of the equipped bench must be freeze to a few hundred grams around 320kg (~310 for the end arms benches, 326kg for the central benches, see slide 13 of VIR-0035A-14).

The following figures show this bench. The drawings of the benches used during the call for tender are attached at the end of this note.



*Figure 1 3d view of the minitower bench. The top surface will be cover by a grid of M6 holes, 25mm spaced. The circular holes are for cables. The ones which will not be used will be covered in order to use this space as any other part of the bench. The primary LVDT coils are also visible on each corner.*

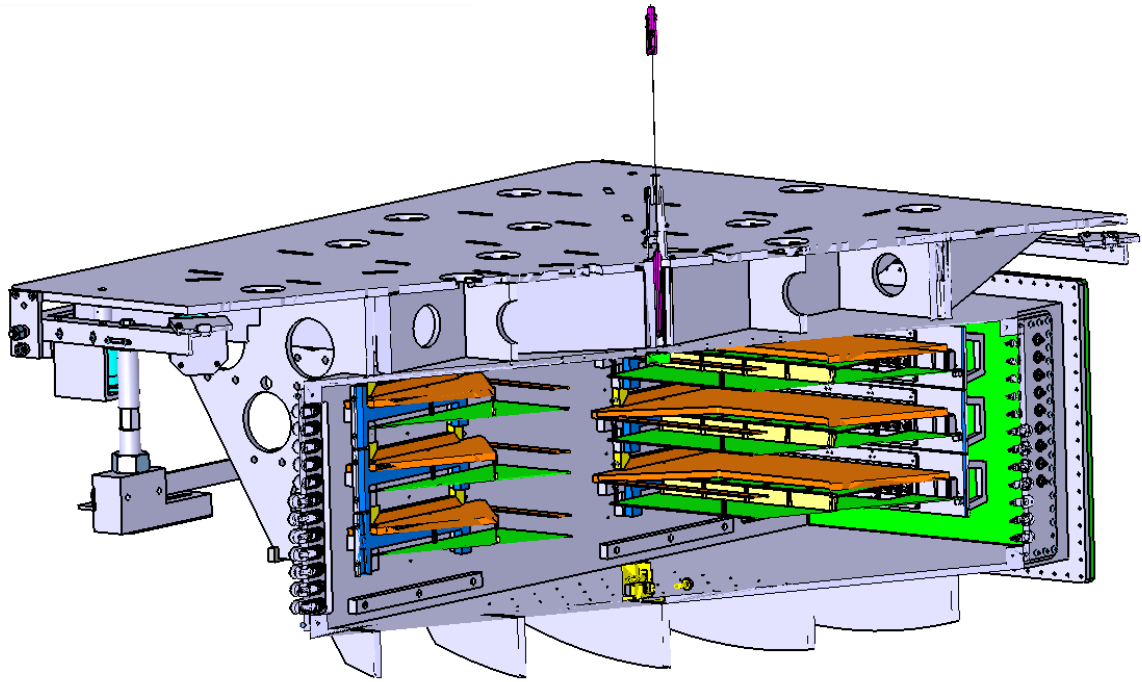


Figure 2 A cross section of the bench. Some of the electronics contained in the bench is visible. The structure holding the coils and the bench is also visible on the left part of the figure.

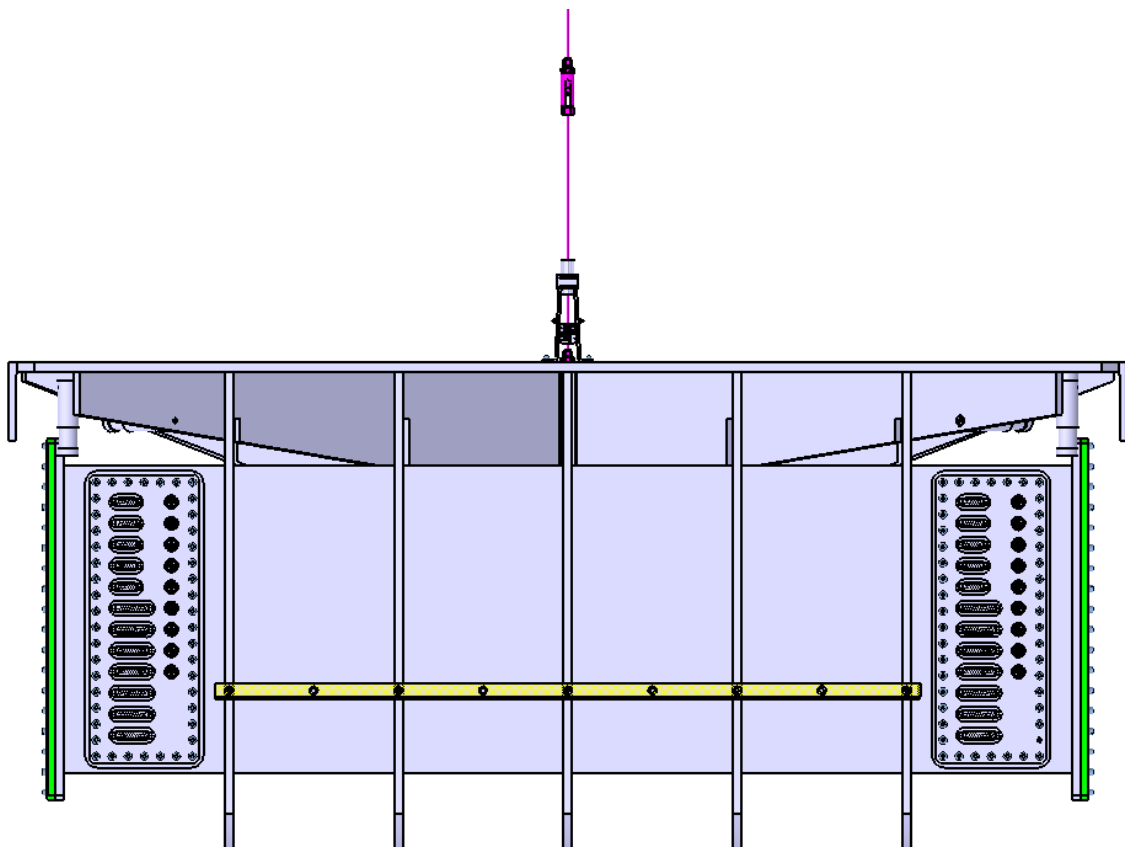


Figure 3 A side view of the bench. The electrical feedthroughs are well visible. The yellowish piece is the rails used to install the bench in the minitower.

## 2 Weight of the equipment put on the benches

The following table gives the summary of the components installed on top of each bench. The weights are mostly estimates made at the time of writing this note. The total expected top weight is less than 80kg.

Device	weight	SDB2		SPRB		SNEB/SWEB		SIB2	
	per unit	quantity	total	quantity	weight	quantity	weight	quantity	weight
PdDC	1,2	4	4,8		0		0		0
PdAC	1,2	7	8,4	2	2,4	2	2,4	2	2,4
PdM	1,2	3	3,6		0		0		0
Quadrant	3	4	12	2	6	2	6	2	6
Galvo	0,5	4	2	2	1		0	4	2
Cameras	2	4	8	4	8	3	6	2	4
Motorized Optic	0,6	26	15,6	6	3,6	3	1,8	2	1,2
Static optic	0,5	4	5	4	2	12	6	12	6
Telescope	-	-		1	20	1	20	1	20
Diaphragms,baffle	-	-	10	-	10	-	10	-	10
Balancing weight	-	-	10	-	10	-	10	-	10
Total optic			79,4		63		62,2		61,6

The following table gives the summary of the components installed inside the electronic air tank. Here again, it is based on estimates. The total expected weight for the electronic is less than 45 kg.

Device	weight	SDB2		SPRB		SNEB/SWEB		SIB2	
	per unit	quantity	total	quantity	weight	quantity	weight	quantity	weight
DAQ box w. heat link	7	4	28	2	14	2	14	2	14
Switch	3,6	1	3,6	1	3,6	1	3,6	1	3,6
RS422 interface	0,5	1	0,5	1	0,5	1	0,5	1	0,5
LVDT: 4 pairs	1	1	1	1	1	1	1	1	1
Drivers picomotors	0,3	14	4,2	4	1,2	8	2,4	8	2,4
Support for pico. Drive	1	2	2	1	1	2	2	2	2
Geophone	3	1	3	1	3	1	3	1	3
Titlmeter	0,2	1	0,2	1	0,2	1	0,2	1	0,2
Cw camera	0,2	1	0,2	1	0,2	1	0,2	1	0,2
Counter weighth	2,2	1	2,2	1	2,2	1	2,2	1	2,2
Total			44,9		26,9		29,1		29,1

Since the weight of the equipped bench is nominally set to 320 kg, the bench itself should not weight more than  $320-80-45= 195$  kg. The CAD estimate of the designed bench (see annex) is 180 kg, fulfilling this limit.

### 3 Vertical tuning of the bench

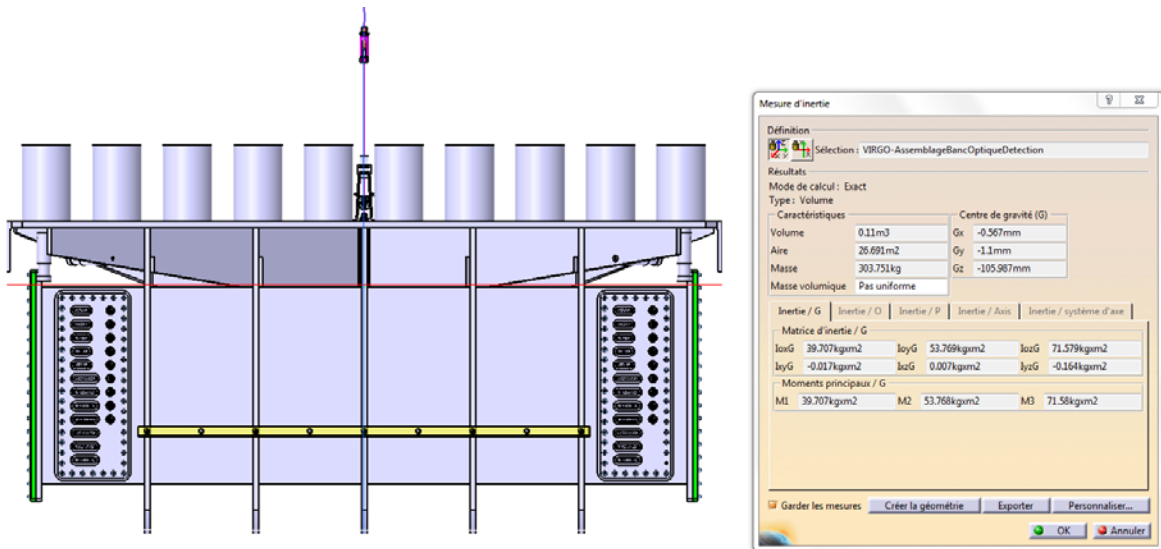
The minitower benches are not attached to a “marionnetta” by three wires like for the injection and detection benches, but are using a single central wire with the goal to provide an additional stage of angular filtering. The target is to have a low oscillation frequency like  $250 \pm 50$  mHz, or similarly a period  $P = 4 \pm 1$  s. The frequency higher bound is to provide enough filtering; the lower one is to stay far enough from the instability.

The oscillation period of a rigid body of mass  $M$  at distance  $d$  between the pivot point and the center of mass is given by

$$P = 2\pi \sqrt{\frac{(I_{cdm} + Md^2)}{Mgd}} \approx 2\pi \sqrt{\frac{I_{cdm}}{Mgd}}$$

Where  $I_{cdm}$  is the moment of inertia.

The moment of inertia of the bench has been estimated by putting 90 kg of dummy load on top of the bench as cylinder visible on the next figure, as well as about 30 kg of electronic. The total weigh of this model is 304 kg, slightly less than the nominal 320 kg. The smallest moment of inertia is  $39.7 \text{ kg.m}^2$ .

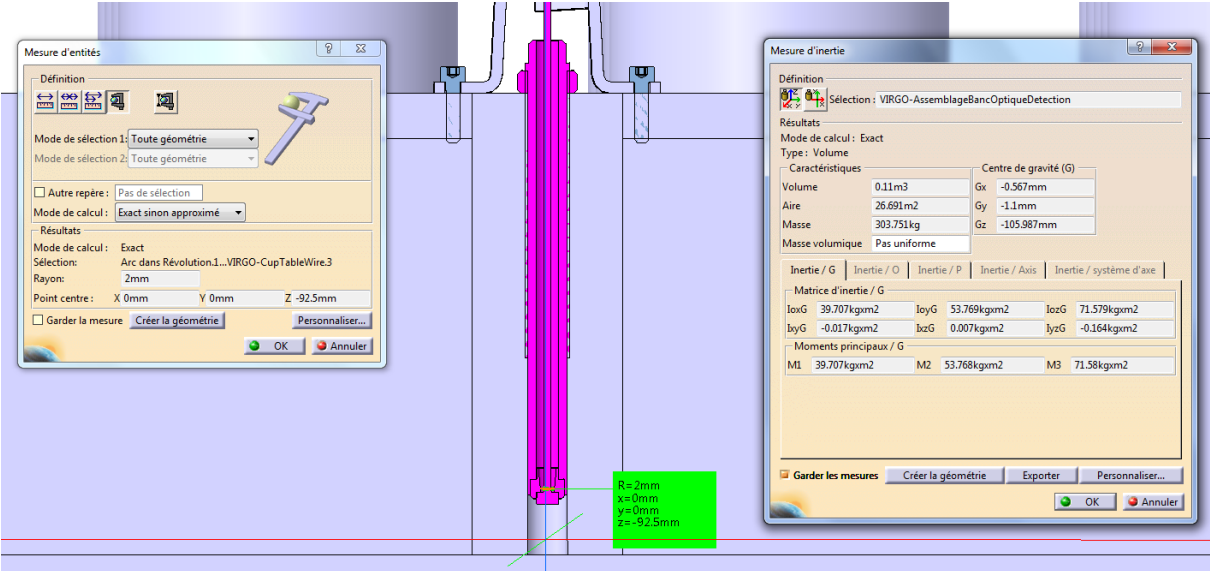


The following table shows the needed distance between the center of mass and the pivot point as a function of the required frequency.

frequency (mHz)	d (mm)
100	5,3
150	11,8
200	21,0
250	32,8
300	47,3
350	64,4
400	84,1

With this configuration, the nominal distance between the center of mass and the pivot point should be 33 mm with a tolerance of 10 to 15 mm. Given the complexity of the bench equipment and cabling, it is difficult to predict exactly the vertical position of the center of mass. Therefore, a very long M12 threaded hole has been made at the center of the bench for the wire holding mechanism. In the above

simple load model, the center of mass is at  $z = -106 \text{ mm}$ , and the pivot point at  $z = -92.5 \text{ mm}$ , 13.5 mm above the center of mass. Of course, there is no problem to raise this pivot point just by unscrewing the wire support (the pink part of the figure). The adjustment margin going down or up is several centimeters. This should be enough since the vertical position of the center of mass should not change to much: for instance moving 10 kg from the electronic air tank to the top of the bench change the vertical position of the center of mass by a centimeter.



## 4 Thermal effects modeling

This section discusses the simple model used to estimate the temperature inside the electronic air tank. As we will see, the use of high conductivity and high emissivity material is mandatory to have enough heat transferred through radiation between the in-vacuum suspended bench and the minitower.

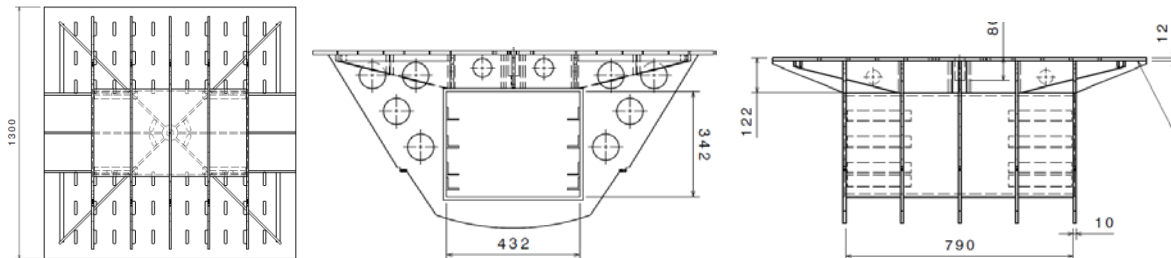
The thermal load due to the electronic is estimated to 300 W in the worse case (SDB2) (see VIR-0198A-14). This section will show that to radiate these 300 W, given the bench geometry, the expected temperature difference between the bench and the minitower wall is 15.8 °C. Assuming a temperature of 21.5 °C for the minitower surface, the temperature of the top of the bench should be around 37 °C, slightly below the maximum operating temperature of the picomotors: 40 °C which are probably the most sensitive devices on the bench.

The temperature gradient inside the bench is estimated to 3.6 °C, giving an estimate maximum temperature of 41 °C for the wall of the electronic air tank. Dedicated heat links will take the heat from the electronic components, to the bench. They are only sketched in this section.

This modeling, which is confirmed by the tests described in the next section, shows that it is feasible to put all the bench components electronic inside the bench in order to avoid a large number of cables running along the seismic isolation and spoiling its performances. However, if this turns out to be a problem, fallback solutions exist. Cooling down the wall of the minitower using for instance some refrigerated water around the minitower is for instance an option. Taking out of the bench the electronic which has the larger power to number of cable ratio like the demodulation electronic is another option.

### 4.1 Bench Geometry

The following bench geometry was used for this modeling. This was an early design with a slightly shorter electronic air tank.



### 4.2 Emissivity

#### 4.2.1 Emissivity of aluminium

The emissivity of the aluminium is low, typically below 10%. This could be easily checked with a thermal camera looking at a warm aluminium plate: its surface temperature is the same as the temperature of the room where the measurement is made, meaning that it is just reflecting infrared light, not emitting much. This is far from what is needed to dissipate the heat coming from the bench electronic. The only well known and easy solution to increase the emissivity is to anodize aluminium. Here again, this could be easily checked with a thermal camera where the observed temperature is the same as the one read by a thermometer, indicating an emissivity close to 100%.

However, anodizing is also well known as a process to be avoided for vacuum components because it creates a porous layer on the surface which traps water. Nevertheless, this is not a permanent leak. Tests have been carried out to check that after some time, the vacuum level reaches appropriate level (see section 5.6), and that pollution is mainly the extra water content. Despite this drawback, this solution will be used.



#### 4.2.2 Emissivity of stainless steel

The effective emissivity of a body is not just given by its own emissivity but depends also of the emissivity of the surface going to absorb the radiation, in our case, the stainless steel walls of the minitower.

The emissivity of material is not accurately provided by the literature since the details of the surface treatment have significant impact on the emissivity. Stainless steel has an emissivity larger than aluminium, but still rather poor around 15 to 20%. There are two ways to easily increase the emissivity of stainless steel:

- **Sand blasting** is increasing the emissivity by at least a factor 2. We measured a 45 to 50% emissivity after sand blasting. This could be understood since sand blasting will create some hole at the surface of the material, increasing its effective surface. In a naive model, were the holes have the shape of half sphere, the surface increase by a factor 2 (this is the ratio between the surface of half a sphere and a disk of same radius), meaning that the emissivity increase by the same amount. This effect should be more or less independent of the size of the material used for sand blasting.
- **Thermal treatment** at high temperature is colouring the surface of steel and increase the emissivity. We checked that a thermal treatment at 400 °C had a limited impact (the emissivity goes only to 20-25%). A treatment at 800 °C gives an emissivity of about 80-85%, much more effective, but more difficult to implement.

The thermal treatment at high temperature has been discarded since it would be a too complex processing on the minitowers. The sand blasting solution is much easier to apply, and anyway much less an issue for the vacuum compatibility than the bench anodizing that is going to be used. This has been tested on a first minitower (see the vacuum tests section).

#### 4.2.3 Procedure to measure the emissivity

The emissivity of small samples has been evaluated by measuring with a thermal camera the effective temperature of several samples put on top of a warm plate of low emissivity (aluminium). The following figure is showing the test setup. The thermometer is measuring the room temperature (24 °C in this case) and the sample temperature (33.4 °C, see the small text just below 24.0)



Figure 4 Picture of the test setup to measure emissivities

The room temperature is evaluated by looking at the wall of the room with the thermal camera (see the left photo of the following figure): 24.3 °C, in agreement with the thermometer. Notice that the aluminum surface on which the sample are placed, despite being at 33°C shows the same temperature as the wall of the room, confirming the very low emissivity of aluminum.

The temperature of the test sample is also measured with the thermal camera by looking at the emissivity of paper glued on top of the samples (central photo): 33 °C, in agreement with the thermometer.

The third photo is showing the surface temperature of the test sample: 28.6 °C. Then the emissivity is computed by doing the ratio of the temperature differences: emissivity= (28.6-24.3)/(33-24.3) = 49.4% in this case, for a sand blasted stainless steel sample. The typical error on this measurement is in the 5 to 10% range, looking at different point of the surface, or redoing the measurement on another day.

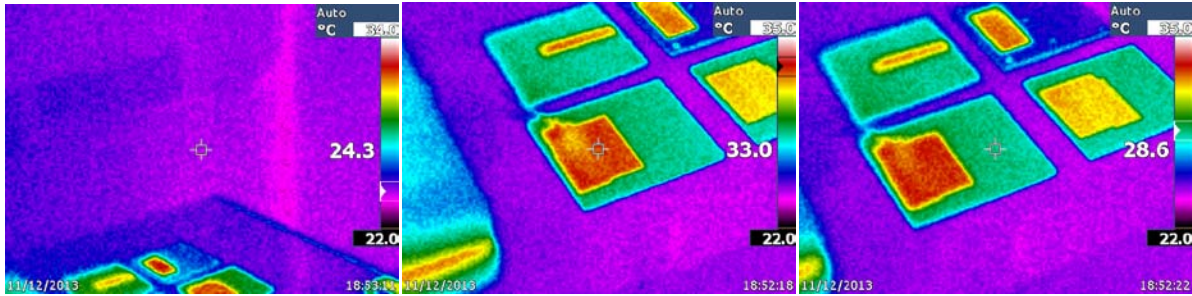
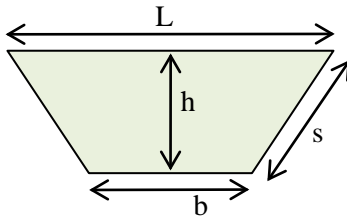


Figure 5 Thermal images used to measure the emissivity of a sand blasted stainless steel sample.

### 4.3 Bench thermal radiation model

#### 4.3.1 Simple bench geometry

For this thermal model, the bench geometry is approximated by a trapezoidal volume of section:  
 $L = 1.3$  m,  $h = 0.5$  m,  $b = 0.5$  m, over a length  $L$



The length of the side is  $s = \sqrt{((L-b)/2)^2 + h^2} = 0.64$  m

The total surface is

$$S = L(L+b+2s) + 2h(L+b)/2$$

$$S = 1.3(1.3+0.5+2*0.64) + 2*0.5*(1.3+0.5)/2$$

$$S = 4.9 \text{ m}^2$$

#### 4.3.2 Effective emissivity

We assume that anodizing will give a 100% emissivity. Once the bench radiation hits the minitower surface it is absorbed with the emissivity of the minitower ( $\epsilon_M$ ) or reflected ( $1-\epsilon_M$ ). The reflected radiation is either send back to the bench where it is absorbed or send to another part of the minitower (fraction  $P_{M \rightarrow M}$ ), were the fraction  $\epsilon_M$  is absorbed and the other part again reflected.

Therefore we get the following fraction of the radiation absorbed by the minitower:

$$\epsilon_{\text{Eff}} = \epsilon_M [1 + (1-\epsilon_M) P_{M \rightarrow M} + ((1-\epsilon_M) P_{M \rightarrow M})^2 \dots]$$

$$\epsilon_{\text{Eff}} = \epsilon_M / [1 - (1-\epsilon_M) P_{M \rightarrow M}]$$

To evaluate  $P_{M \rightarrow M}$ , we ran a 2d numerical simulation, assuming than the bench is of infinite length, taking the minitower diameter of 1.4 m. We got  $P_{M \rightarrow M} = 50\%$ . This is anyway close to the ratio between the bench surface ( $4.9 \text{ m}^2$ ) and the minitower inner surface (a little less than  $10 \text{ m}^2$ , we will use  $9.8 \text{ m}^2$ ).

If we combine this result with the 45%  $\epsilon_M$  emissivity for sand blasted stainless steel we end up with an effective emissivity of  $\epsilon_{\text{Eff}} = 0.45 / (1 - (1-0.45)0.5) = 62\%$ .

Remark: for raw stainless steel with 20% emissivity, the effective emissivity is only  $\epsilon_{\text{Eff}} = 33\%$ .

### 4.3.3 Bench temperature

The power radiated by a surface  $S$  of emissivity  $\epsilon_{\text{Eff}}$  at temperature  $T$  is

$$P_{\text{rad}} = \epsilon_{\text{Eff}} S \sigma T^4 \quad \text{with } \sigma = 5.67 \times 10^{-8} \text{ W m}^{-2} \text{ K}^{-4} \text{ the Stefan-Boltzmann constant.}$$

At equilibrium, the radiated power by the bench at temperature  $T_1$  must be equal to the dissipated power  $P$  plus the received power from the minitower radiation which is at temperature  $T_0$ :

$$\epsilon_{\text{Eff}} S \sigma T_1^4 = P + \epsilon_{\text{Eff}} S \sigma T_0^4$$

therefore

$$T_1 = T_0 [1 + P/(\epsilon_{\text{Eff}} S \sigma T_0^4)]^{1/4} \quad (1)$$

For  $T_0 = 294 \text{ K}$ ,  $S = 4.9 \text{ m}^2$ ,  $\epsilon_{\text{Eff}} = 62\%$ ,  $P = 300 \text{ W}$ , we get  $dT = T_1 - T_0 = 15.8 \text{ K}$ .

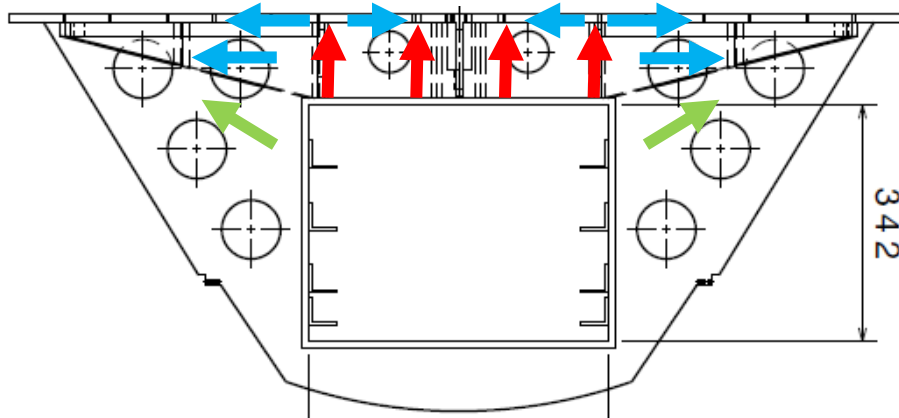
Notice that in first approximation, this temperature difference is proportional to the radiated power.

If we were using plain aluminum, with a typical 5% emissivity, the temperature difference would be  $dT = 119 \text{ K}$ , highlighting the need for anodizing. Similarly, without sand blasting, the effective emissivity will be 33%, the temperature difference  $dT = 28 \text{ K}$ , translating to a bench surface at about  $50 \text{ }^\circ\text{C}$ , too high for picomotor operations.

### 4.4 Estimation of the temperature gradient inside the bench

Some of the surface of the air tank could directly radiate heat to the minitower inner surface. But a fair fraction of the heat will first propagate through the bench structure before reaching the radiating surface, like the top of the bench. This will create a temperature gradient between the electronic air tank and the radiating surface.

Let's try to do a simple estimate of the temperature gradient between the air tank and the top surface of the bench. For this naïve model, we assume that half of the power, i.e.  $150 \text{ W}$ , will follow this path in two steps sketched in the following figure:



**Step 1 (red arrows): going from the top of the electronic air tank to the top of the bench.**

The upper part of the air tank is connected to the top surface by 5 large lateral ribs, plus 2 diagonals and 1 along the axis. All ribs are 10mm thick. The total cross section is therefore:

$$S = (5 \cdot 0.450 + 2 \cdot 0.45 \cdot 1.414 + 0.8) \cdot 0.01 = 0.043 \text{ m}^2.$$

Since the thermal conductivity of aluminum 6060 is  $C = 209 \text{ W/m/K}$ , and the travel path of  $L = 110 \text{ mm}$ , the thermal resistance of this connection is:

$$R = L/(S \cdot C) = 0.11 / (209 \cdot 0.042) = 0.0122 \text{ K/W}$$

For a  $150 \text{ W}$  flux, this translate to

$$dT = 1.8 \text{ K}$$

**Step 2 (blue arrows): diffusing inside the top surface.**

Once the heat reaches the top surface, it must travel on average something like 15 cm from the rib to the radiating surface. The footprint of the air tank on the top surface has a perimeter of  $2 \times (0.45 + 0.8) = 2.5$  m. Since the thickness of the bench is 12 mm, this gives a cross section of  $0.03$  m<sup>2</sup>. This cross section is roughly doubled by the ribs which carry also heat from the center of the bench to the outside. This translates to a temperature difference of  $dT = 1.8$  K

**Summary:** The total temperature difference is therefore  $1.8 + 1.8 = 3.6$  °C. This is probably an upper limit since other paths like the one sketch with the green arrows have been neglected. This relatively small value indicates that a uniformed bench temperature could be used in first approximation when doing the radiating model of the bench.

This temperature gradient shows also that the use of aluminum, compared to stainless steel is mandatory. Stainless steel has a thermal conductivity smaller by an order of magnitude, meaning thermal gradient would be 10 times larger. Furthermore, to keep the weight constrain, the thickness of the ribs would be 2 to 3 times smaller, increasing further the thermal gradient in case of stainless steel use.

**4.4.1 Temperature of the walls of the air tank**

Adding the 3.6 °C difference to the  $dT$  of 15.8 °C from the bench surface to the minitower which is assumed to be at 21.5 °C, we get 41 °C as temperature of the inner wall of the air tank. This is acceptable for the operation of regular electronic components like the network switch which requires less than 50 °C. However, the heat coming from the most powerful electronic components will have to be transported to the air tank wall in an efficient way to avoid overheating. Therefore, heat guides will be installed to connected components like ADC, FPGA and amplifier to the air tank walls. These heat links will be connected by thermal foam to the electronic components, and by a “pincer” on the walls of the air tank.

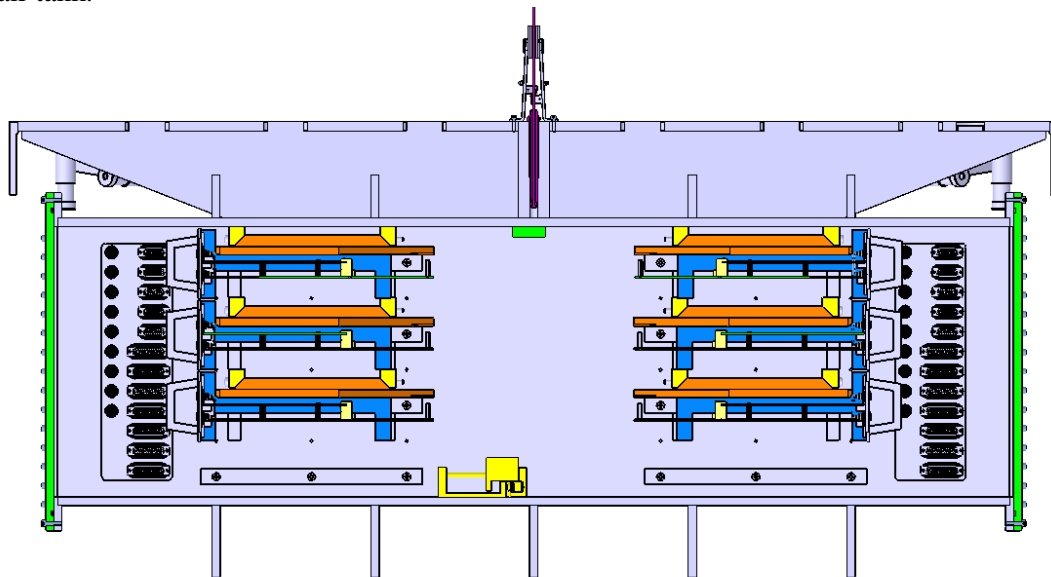


Figure 6 Cross section of the minitower bench, showing the DAQbox and their heat link (orange part). The blue and yellow parts are the pincer. The blue part is attached to the wall on which threatened holes have been made.

**4.4.2 Thermal gradient inside the air tank shell or minitower shell:**

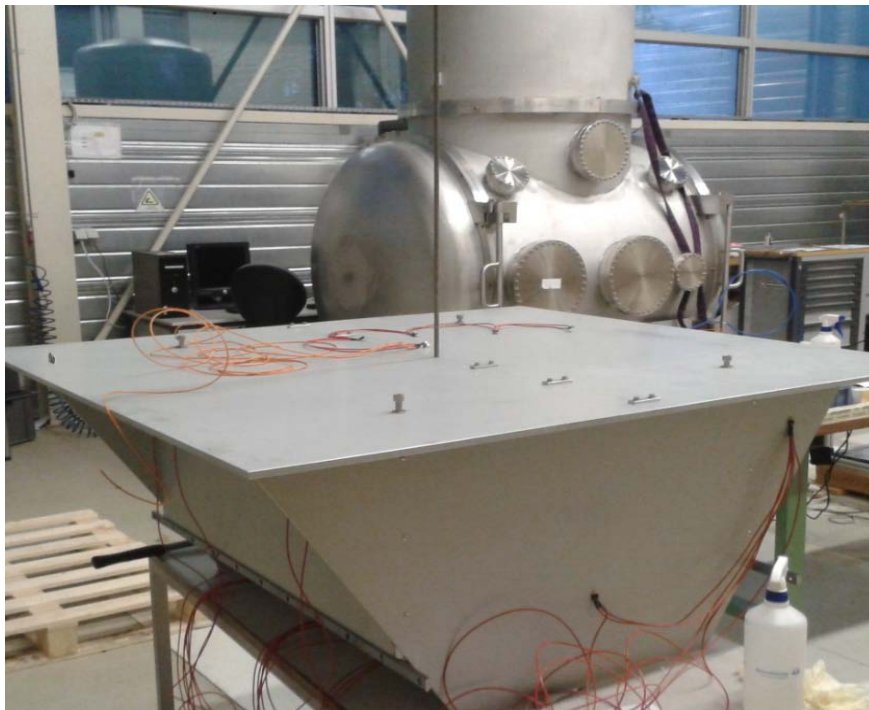
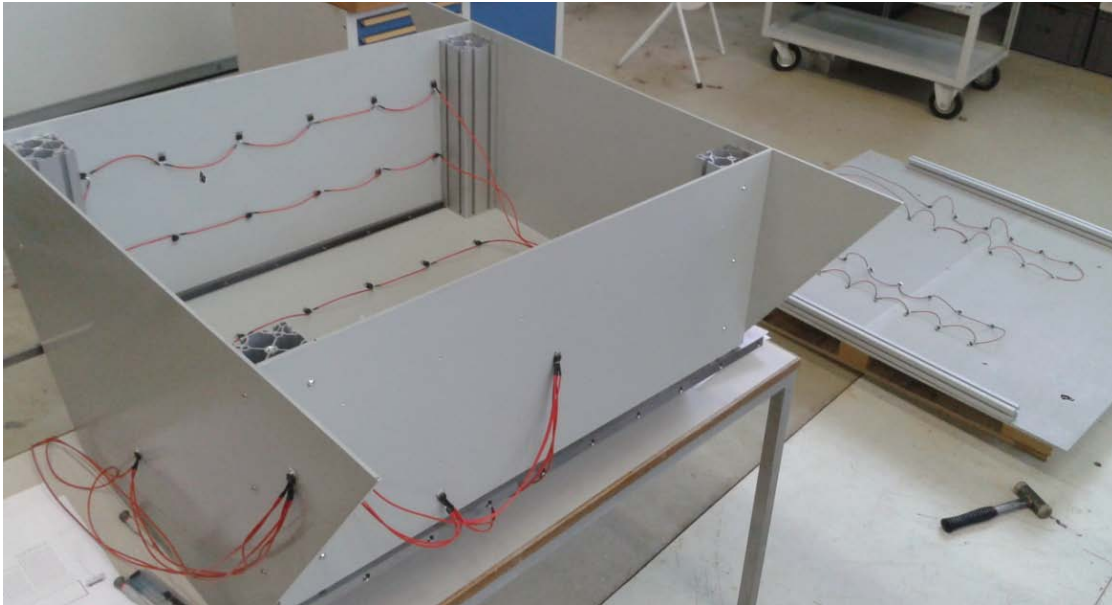
The 300 W will have to go through the walls of the air tank (aluminum, 10 mm thick over  $1.6$  m<sup>2</sup>) and the minitower (stainless steel, 8 mm over about  $8$  m<sup>2</sup>). Given the thermal conductivity of aluminum 209 W/m/K and stainless steel, 17 W/m/K, the thermal gradients in these walls are 0.01 °C for the air tank and 0.02 °C for the minitower, and therefore negligible.

## 5 Heat transfer test

To validate the thermal model a “dummy” bench has been build and tested under thermal load inside the minitower. The sections described the tests carried on.

### 5.1 Dummy bench used for this test

The dummy bench was made of a few plates of anodize aluminium, to replicate the volume of the suspended bench. The thickness of the anodized layer was about 10  $\mu\text{m}$ . No sealing step was made at the end of the anodizing process. The following figures present this bench. Resistors were installed inside the “box” to be able to warm it, while temperature sensors where attached on the outside.



*Figure 7 Images of the dummy bench*



This dummy bench is slight smaller than the real bench, leading to a radiating surface 10 to 20% smaller than the final one (see Figure 1).

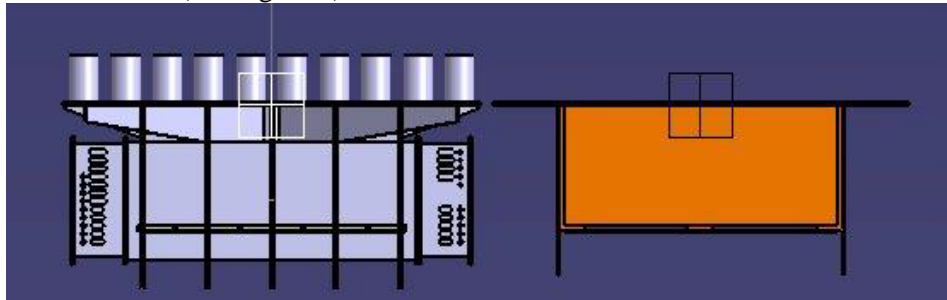


Figure 8 Comparing the real bench size (left) to the dummy bench (right).

### 5.2 Installing the dummy bench in the minitower

The bench was put inside the minitower and suspended to a rod. Given the typical observed temperature difference between the bench and the tower: ( $dT = 23 \text{ K}$ ), the rod radius ( $r = 8 \text{ mm}$ ), its length ( $L = 30 \text{ cm}$ ), the thermal conductivity of steel ( $C = 46 \text{ W/m/K}$ ), the expected heat leak trough the suspending rod is  $0.18 \text{ W}$  ( $\pi r^2 C dT/L$ ) and therefore negligible.



### 5.3 Power dissipated in the dummy bench

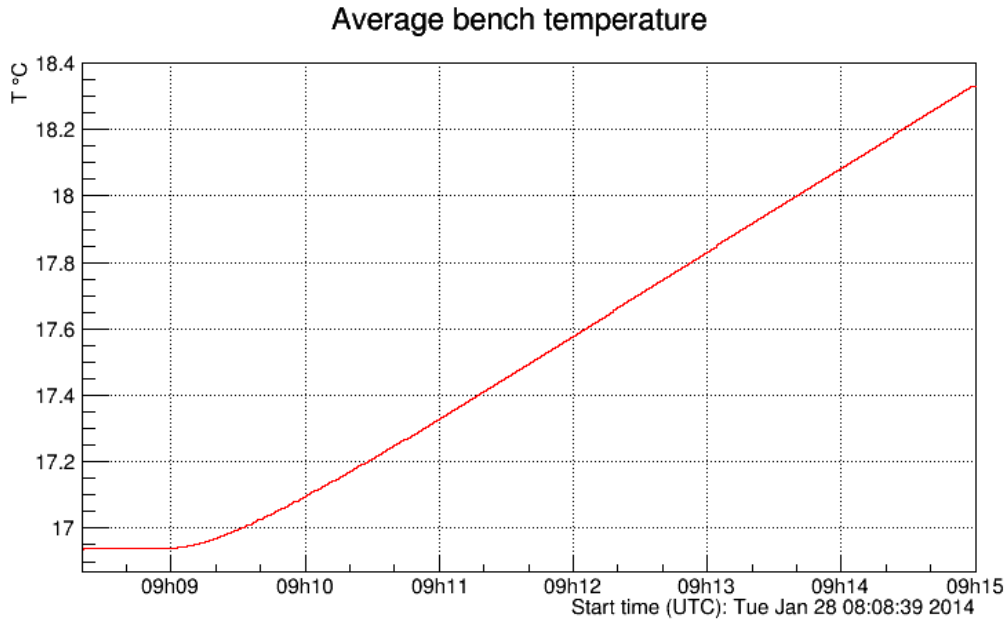
The dummy bench was warmed by a current of around 2 Amperes going through five set of twelve  $1 \Omega$  resistors. The reading of the currents and voltages applied lead to a total dissipated power of 232 W for the tests before minitower sand blasting and 251 W after sand blasting.



Figure 9 Reading of the power supply for the April 11 test .The 24V or so are used to power the resistors. The 5V are used by the temperatures probes.

Given the weight of the dummy bench (65 kg, from the dimension of the bench), the thermal capacity of aluminum (900 J/K/kg), the expected time to warm up the bench by 1 degree is  $65 \cdot 900 / 232 = 252$  seconds, assuming that thermal exchange are negligible as we could expected at the beginning of the warm-up.

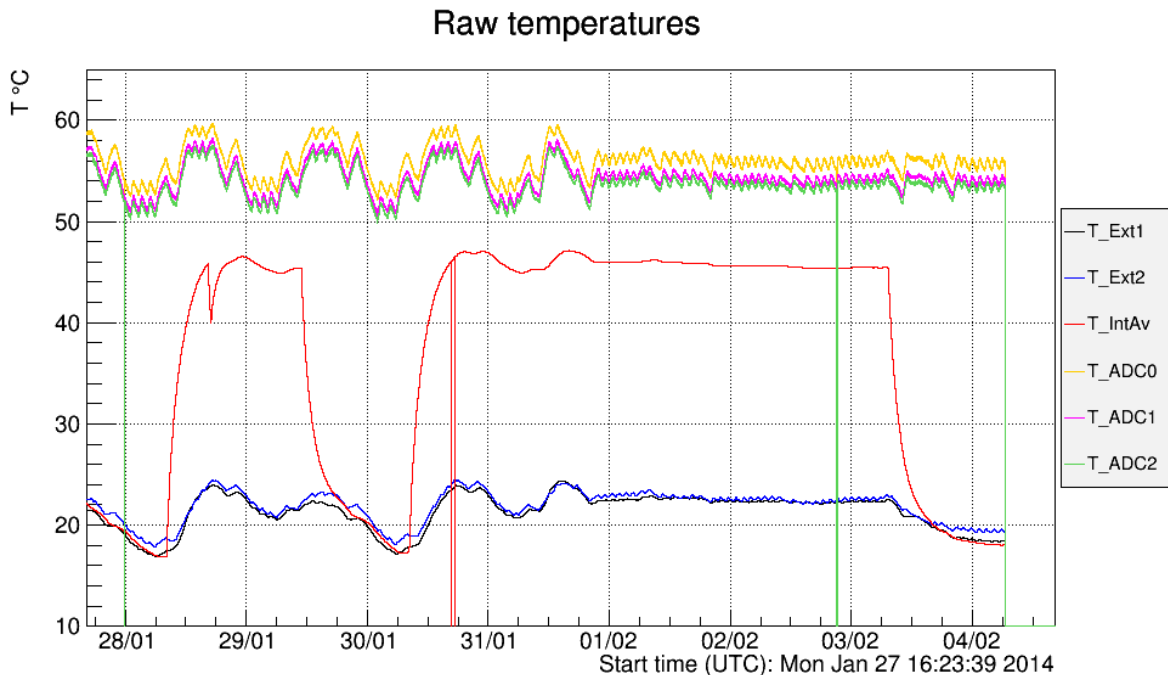
The following figure shows the observed average temperature of the bench during the first few minutes of the warm-up. We observed that 249 seconds are needed to reach a 1 degree difference (going from 17 °C to 18°C), in good agreement with the expectation, and therefore confirming the value of the dissipated power.



## 5.4 Test before minitower sand blasting

### 5.4.1 Observed temperatures

The following figure presents the raw temperatures during the few days of the test.



The average bench temperature is shown as the red trace. There were two periods of bench warming,

well visible. During the first one, the power was cut for a few hours, explaining the deep on the middle of January 28.

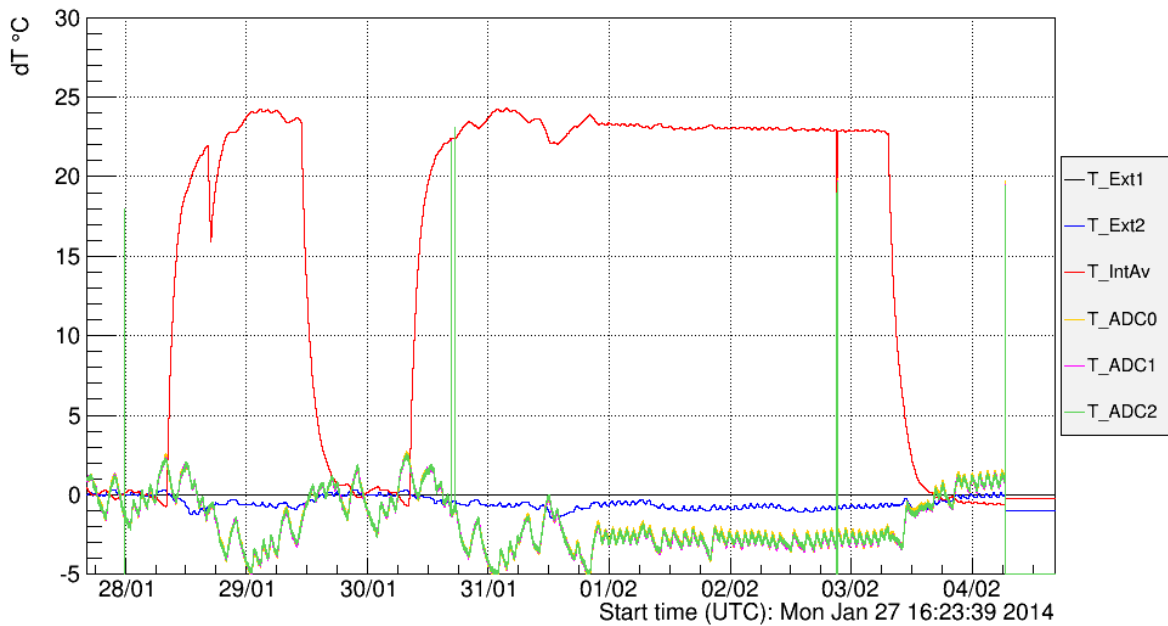
The yellow, purple and green traces show the temperature of the ADCs. This is an information useful to monitor the variations of the room temperature, beside their large offset due to the continuous operation of the ADC. In addition to the short term variation due to the on/off of the room heaters, a day/night effect is visible up to Feb. 1<sup>st</sup> when the set point of the room heating system was change to have the same values for day and night.

The blue and black traces display the temperature of the minitower body, measured on each side of the chamber. They follow the day/night effect and an additional offset is visible when the bench is heated.

To better view the temperature variations and especially to measure the temperature difference between the bench and the minitower, the following figure presents the offset to one of the minitower temperatures, removing also an initial offset taking a few hours after start of the measures. The measure temperature difference between the bench and the minitower is between 23 and 24 K.

The minitower is about 2.5 K warmer than the room, in order to evacuate the power. This heat transfer is mostly through convection, since the expected radiated power given the surface of the chamber (about 10 m<sup>2</sup>), the emissivity of stainless steel (20%) and the 2.5 K temperature difference is expected to be 29 W. There is therefore no need to try to optimise the emissivity of the external surface of the minitower.

**Temperatures relative to minitower**



#### 5.4.2 Expected temperature difference

The dummy bench is slightly smaller than the real bench. Its overall external surface is estimated to about 4.5 m<sup>2</sup> to be compared to the ~ 4.9 m<sup>2</sup> for the regular bench as described in section 6.4. Therefore the expected effective emissivity is slightly different, around 0.35, using an emissivity of 1 for the bench, 0.2 for the stainless steel of the minitower and a 9.8 m<sup>2</sup> for the inner surface of the tower (effective emissivity  $\epsilon_{\text{Eff}} = 0.2/[1-(1-0.2)*(9.8-4.5)/9.8] = 0.35$ ).

Using the equation of section 4.3.3,  $dT = T_0 [1+P/(\epsilon_{\text{Eff}} S\sigma T_0^4)]^{1/4} - T_0$  with  $T_0 = 294\text{K}$ , we get an expected temperature variation  $dT = 22.6\text{ K}$

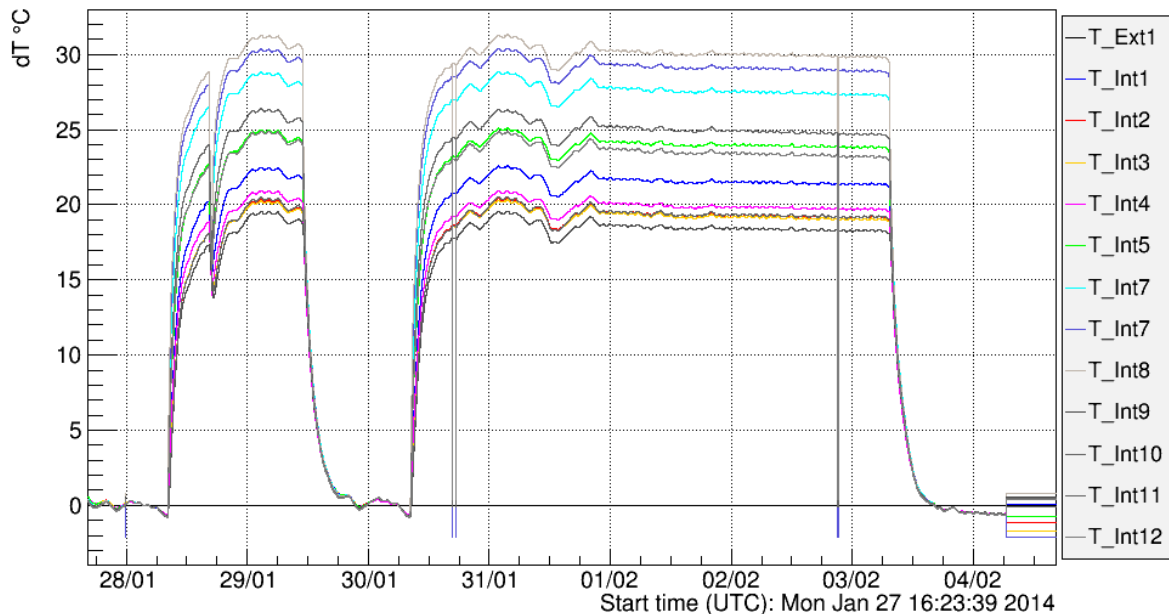
The measured difference is around 23.5 K, in fair agreement with the expectation given the simplicity of our model.



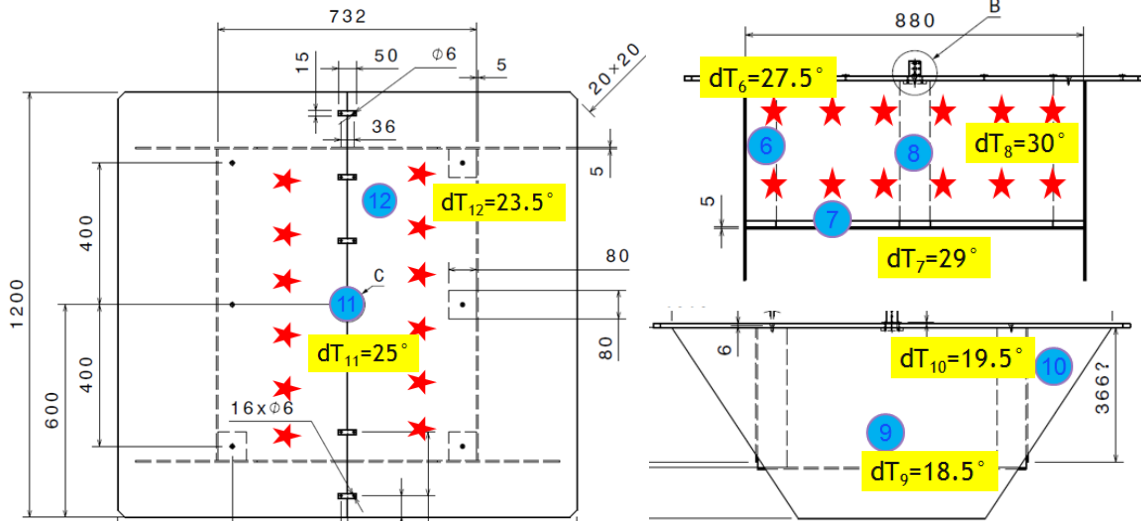
### 5.4.3 Temperature gradient inside the dummy bench

Actually twelve probes are used to monitor the bench temperatures. The following figure shows all the values, relative to the minitower temperature. Their respective offsets have also been subtracted.

Bench temperatures relative to minitower



The typical temperatures offset have been reported hereafter on the sketch of the dummy bench. The warmest locations are the one on the side of the bench, where the solid angle for radiating the power is limited due to the top of the bench. The thickness of the material used for the real bench is expected to be 2 to 3 times more, which therefore should reduce the temperature variation to about 3 to 5 K for different points of the bench, in agreement with the value discussed in section 4.4.

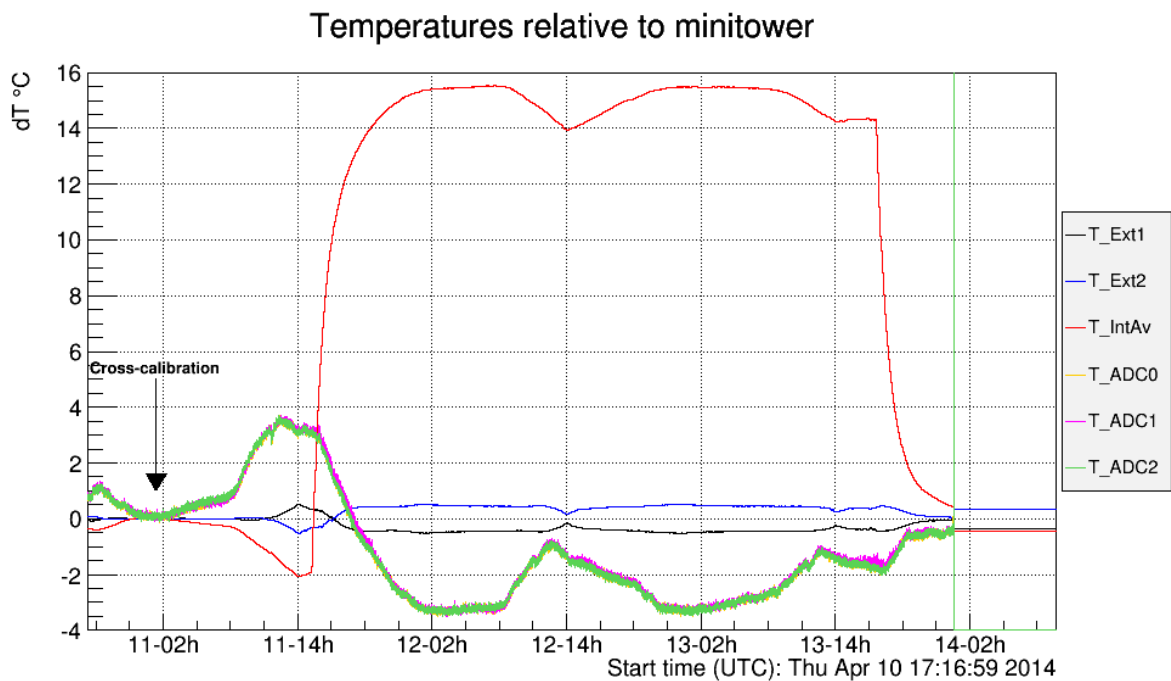
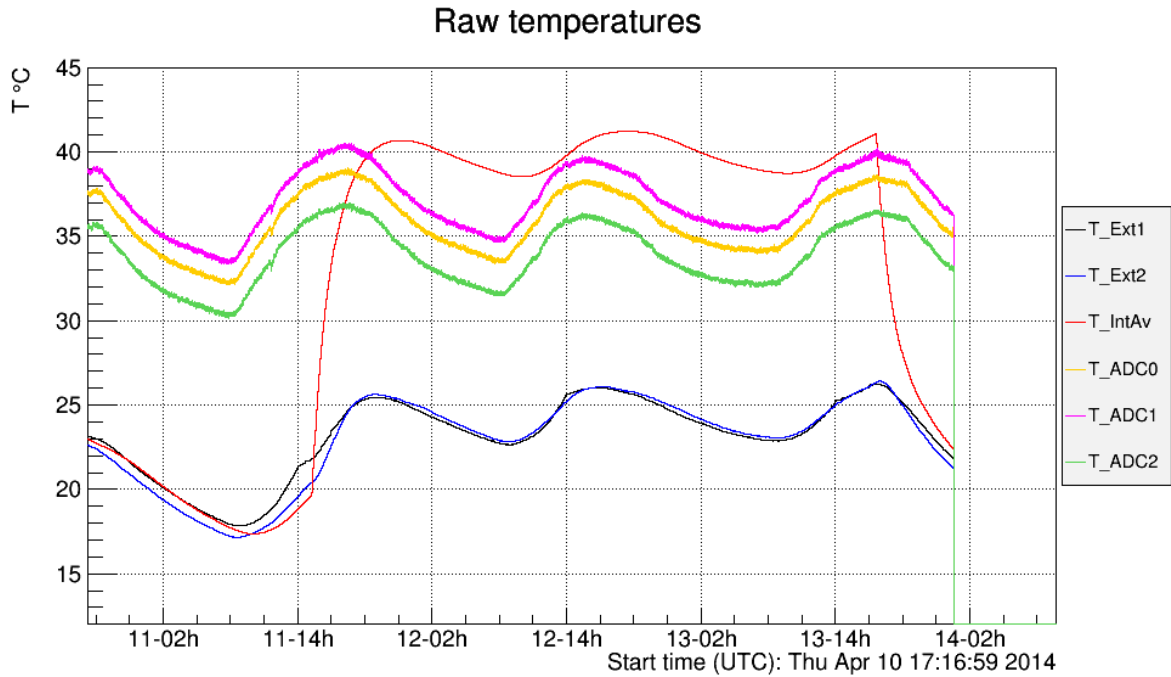


## 5.5 Test with sand blasted minitower

### 5.5.1 Observed temperatures

The two following figures present the raw temperatures during the few days of the test as well as the differences, as for the case before sand blasting.

For this test, the ADC boards are in an air fan cooled crate, reducing their temperature compare to the plot made before the minitower sand blasting. Since during the time of the test, the weather was pretty good, the heating of the hall was switched off, which removed the short term temperature variations but add larger amplitude day/night changes.



*Figure 10 Temperature of the dummy bench with 250 W in a sand blasted minitower.*

After sand blasting, the emissivity of stainless steel is expected to go from 20% to around 45%. This translate to an expected effective emissivity of 64% ( $0.45/[1-(1-0.45)*(9.8-4.5)/9.8]=0.64$ ), and a temperature difference of  $dT = 14.1$  K for 251 W of power with this test. This is a good agreement with the observed temperature difference of about 15 °C, validating the thermal model used.

The minitower remains about 2.5 °C warmer than the room, in order to evacuate the power. This is unchanged compared to the measurement with the non sand blasted minitower since this treatment was only for the inside of the chamber. It highlights that further cooling down of the bench could be achieved by cooling the minitower body with refrigerated water for instance.

## 5.6 Impact of anodizing and sand blasting on the vacuum quality

Anodizing is known to be a bad process for vacuum components, since it acts like a sponge and traps for instance water which is slowly released. This section described the measurement made.

### 5.6.1 Minitower pressure

The Following left top figure is presenting the minitower pressure during the test with the anodized dummy bench minitower before the minitower sand blasting. The bottom left figure is presenting the temperature of the dummy bench. As expected, the pressure is increasing when the temperature increase.

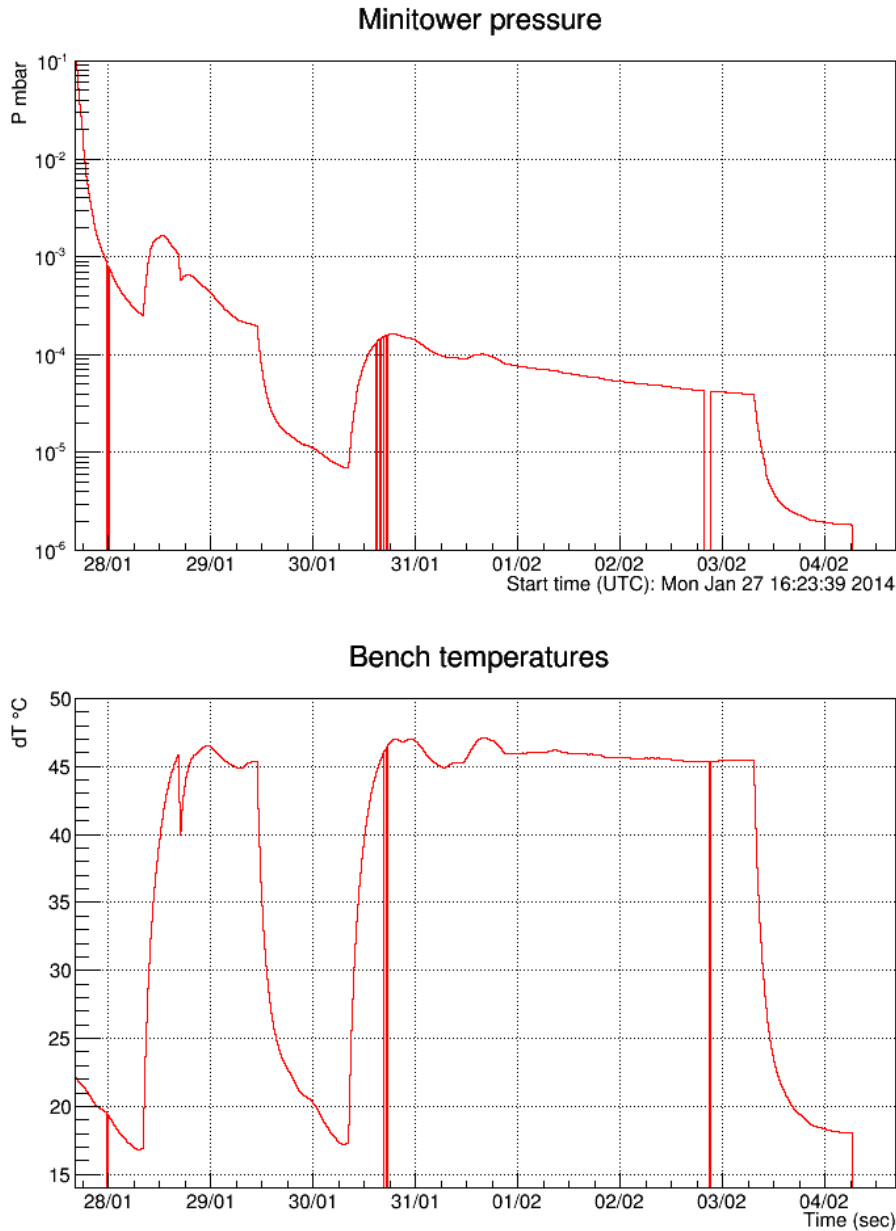


Figure 11 Correlation between minitower pressure and bench temperature

Figure 12 compares different pump-downs, all made with the same 200 l/s turbo pump.

With an empty minitower,  $10^{-5}$  mbar is reached after a couple of hours.

With the empty but sand blasted minitower, after the initial pump down, the pressure is a factor 3 to 5 higher, due to the increase of surface created by the sand blasting in order to increase the minitower emissivity.

With the anodized dummy bench, the pressure is two to three orders of magnitude higher, corresponding to the much larger effective surface to trap water. The pressure does not depend on the state of the minitower (sand blasted or not), since the bench surface is the dominant contribution. The bench temperature due to the on/off of the heating or the day/night effect is also well visible in the tails of the curves. Nevertheless, the pressure is decreasing with time, reaching a few  $10^{-5}$  mbar after typically a week of pumping. This is an acceptable value since these benches will be separated from the main Virgo vacuum by windows, and most of the time, only primary vacuum will be used.

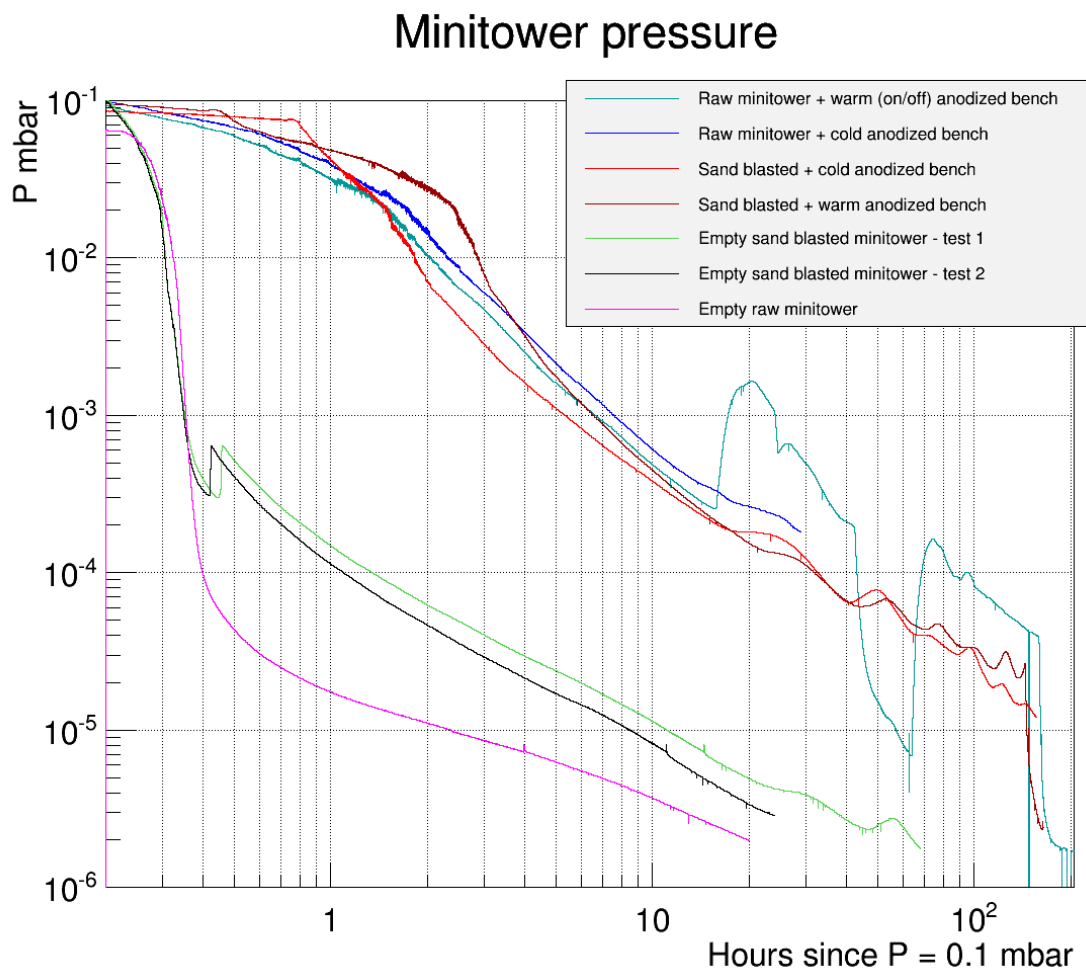


Figure 12 Summary of the pump down. The glitches around  $4 \cdot 10^{-4}$  mbar in the case of the empty sand blasted minitower are due to a change of gauge scale

It is interesting to notice that the integral of the pressure during the pump down with the warm bench + sand blasted minitower is 540mbar.s. If we multiply that by the 200l/s of the pump, we get about 110 l of gas at atmospheric pressure. Assuming this is water, this translates to about 88 g. If we spread this on the about  $8\text{m}^2$  of anodized surface, we get an  $11\mu\text{m}$  thick layer, in agreement with the thickness of the anodized layer which is supposed to act as a sponge and be full of water.

### 5.6.2 Quality of the vacuum: RGA spectrums

The following figures show, for reference, spectrums taken in different conditions. In all cases, water is dominant.

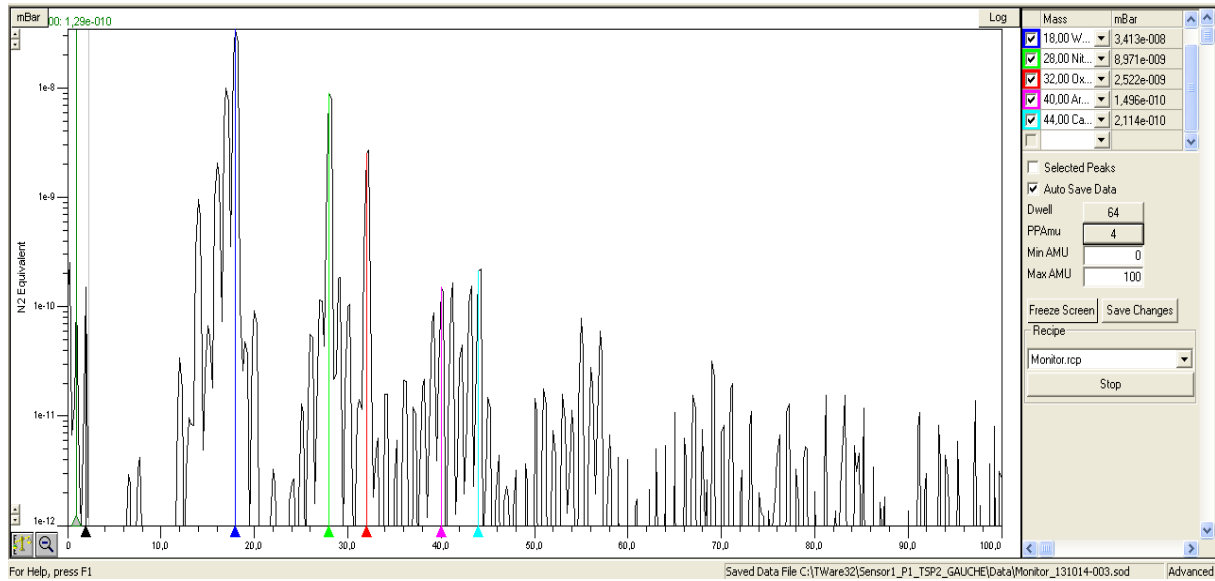


Figure 13 RGA spectrum taken after 6 days of pumping of an empty raw minitower (before sand blasting). The total pressure was  $4.5 \cdot 10^{-7}$  mbar.

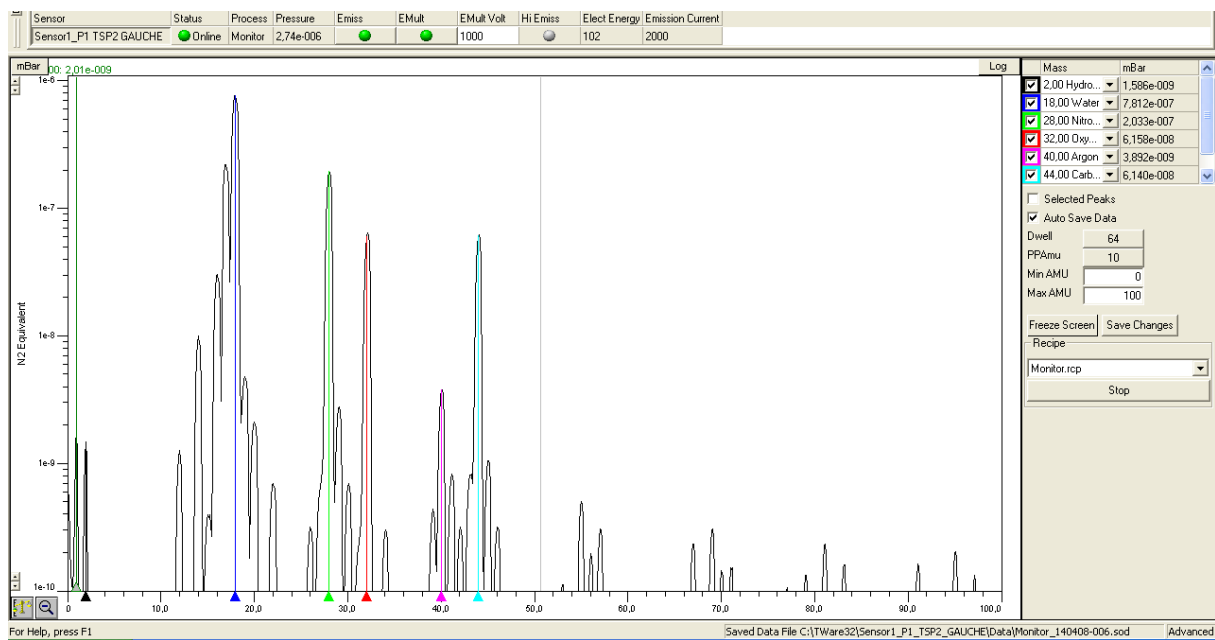


Figure 14 RGA spectrum of the empty sand blasted minitower after 24 hours of pumping. The total pressure was  $3 \cdot 10^{-6}$  mbar. The spectrum is not very different from the raw minitower.

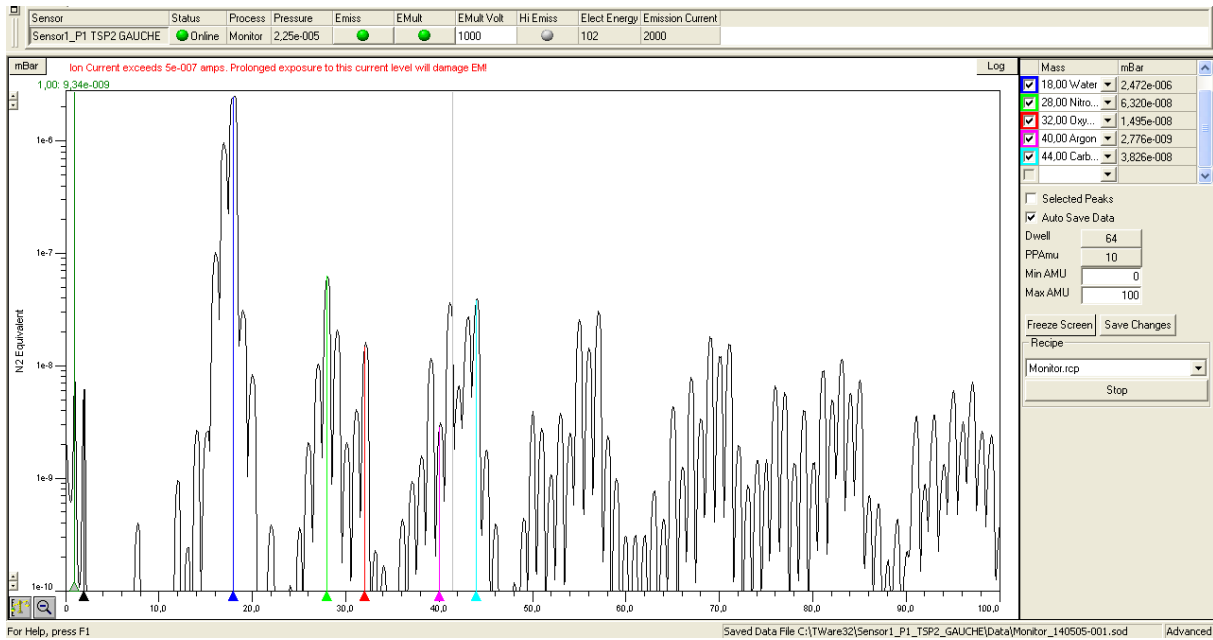


Figure 15 RGA spectrum after 6 days of pumping with the dummy bench heated to around 40°C in the sandblasted minitower. The total pressure was  $2.2 \cdot 10^{-5}$  mbar.

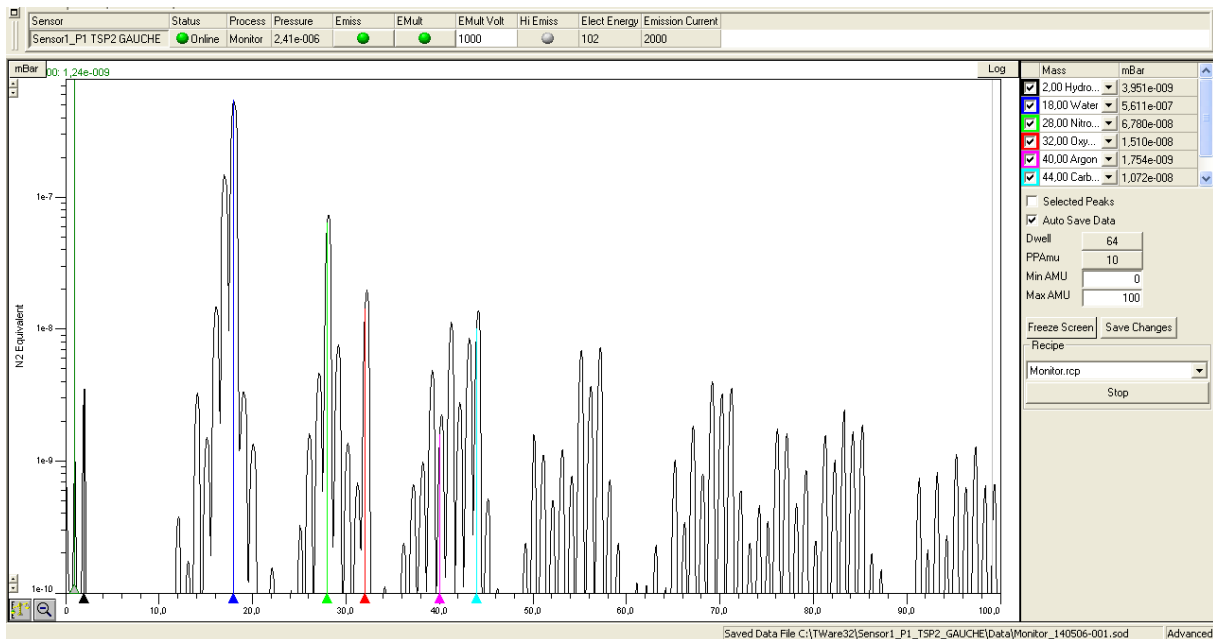


Figure 16 RGA spectrum taken about a day after the one of Figure 15 (with a dummy bench). During the last day, the heating was turned off to cool the bench to room temperature. The total pressure is  $2.4 \cdot 10^{-6}$  mbar.

## 6 Finite element modeling

### 6.1 Geometry of the bench used

The following figures are showing the geometry of the bench used for the finite element modelling. The bench was loaded with the equivalent of about 90 kg on the top surfaces, and some dummy mass to simulate the weight of the electronic. The modelling was not made with the final bench geometry, but the differences are rather small: the main one was that the electrical feedthroughs which were on a removable section, while they have been included in the body of the electronic air tank, making the bench slightly lighter. The number and size of the ribs were not changed since this study and correspond to the final bench configuration.

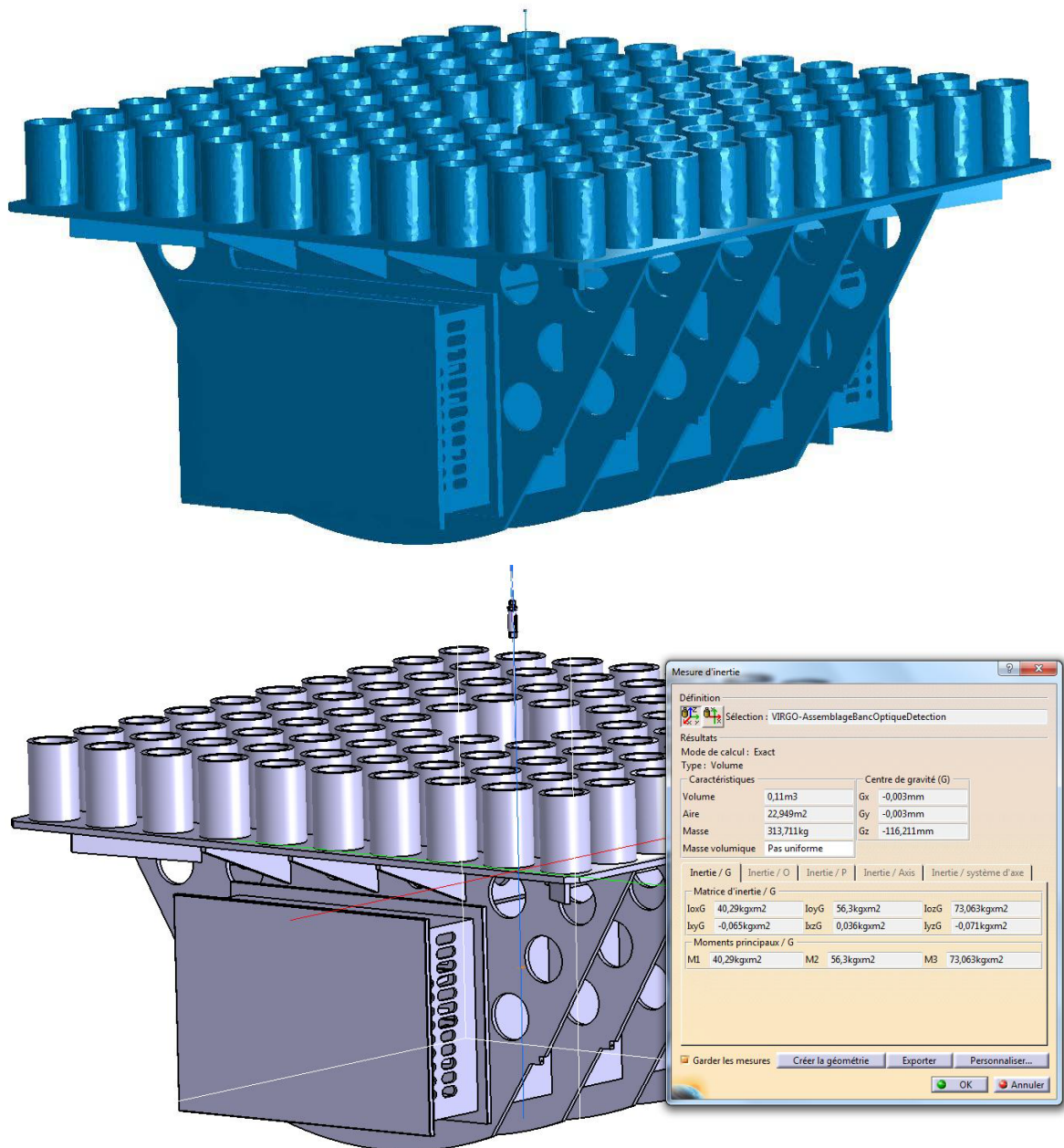
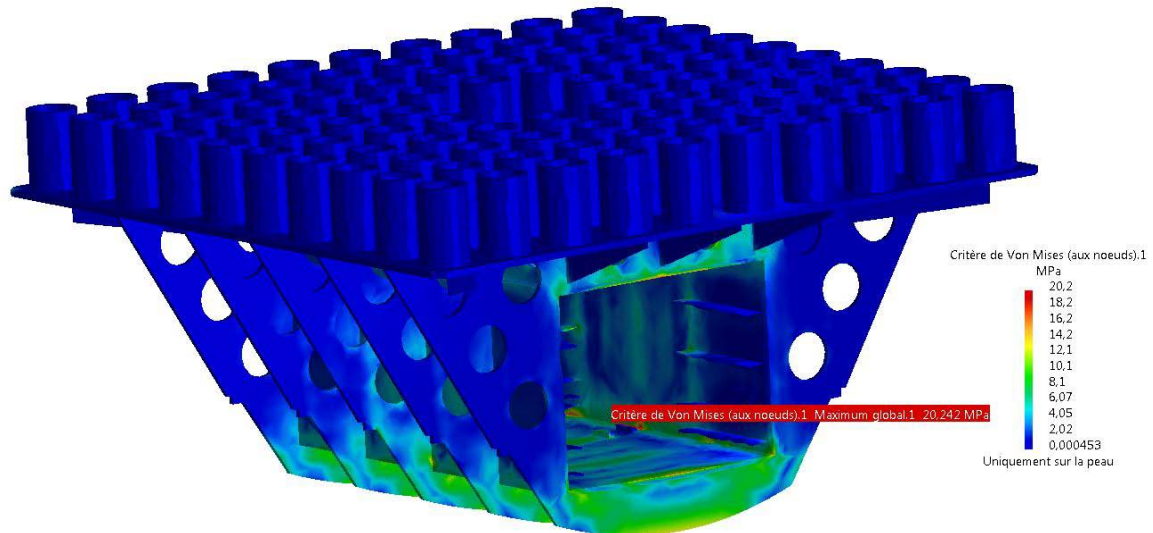


Figure 17 Bench configuration used for the finite element modelling.



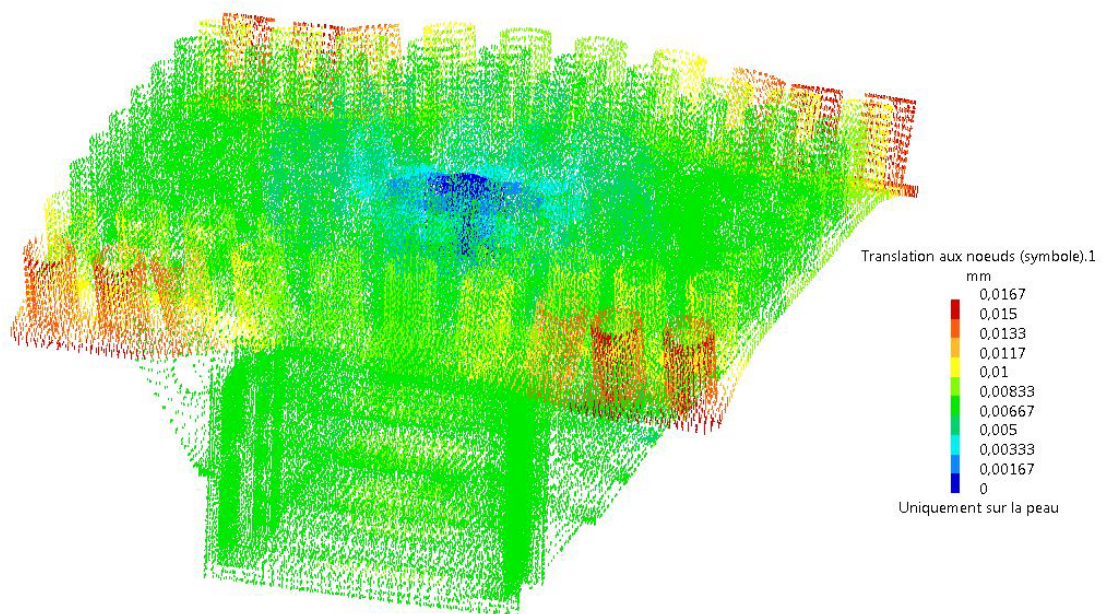
## 6.2 Stress of the electronic air tank walls

The effect of putting the bench under vacuum, keeping the electronic air tank at atmospheric pressure has been computed. The following figure is showing the result. Thanks to the thick walls and reinforcing ribs, the maximum stress is 20 MPa, well below the maximum allow stress (for aluminium 6060, the proof stress is 185 MPa).



## 6.3 Bench deformation due to its weight

The following figure is showing the bench deformation due to its weight once it is suspended to the central suspension wire. The maximum deformation is 16.7  $\mu\text{m}$  on the corner of the bench.





## 6.4 Normal modes

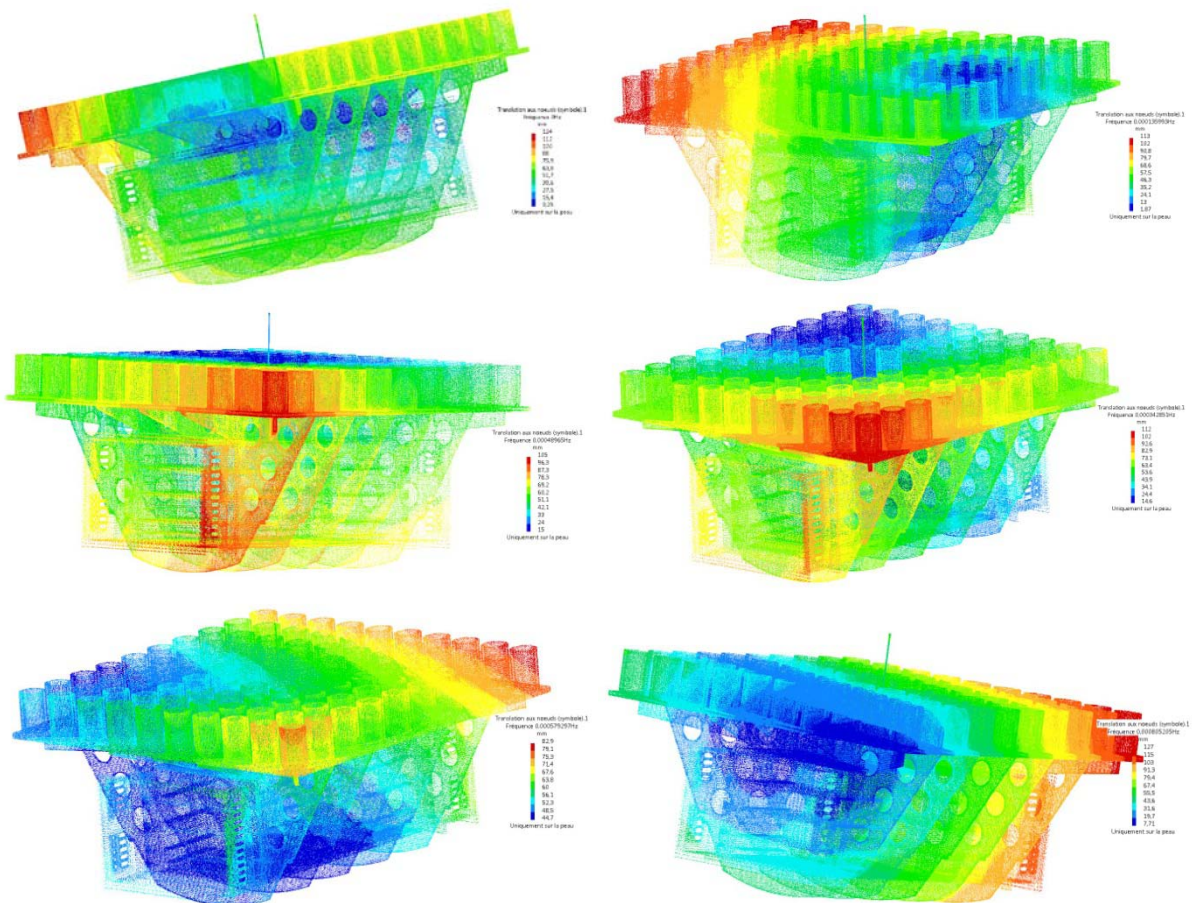
The normal modes have been searched. For this study, the bench was attached by its suspension wire. The following table is giving the list of the first 16 modes.

Nombre de modes	Fréquences (Hz)
1	0
2	0,000135993
3	0,000342851
4	0,00048965
5	0,000579297
6	0,000805205
7	7,76281
8	7,77452
9	49,5849
10	49,6586
11	140,659
12	140,864
13	193,692
14	204,616
15	210,649
16	217,507

Actually, the first 12 modes are not real modes of the bench body, as it can be seen in the next subsections. The first real mode of the bench body is at 193.7Hz, well above the required 150 Hz.

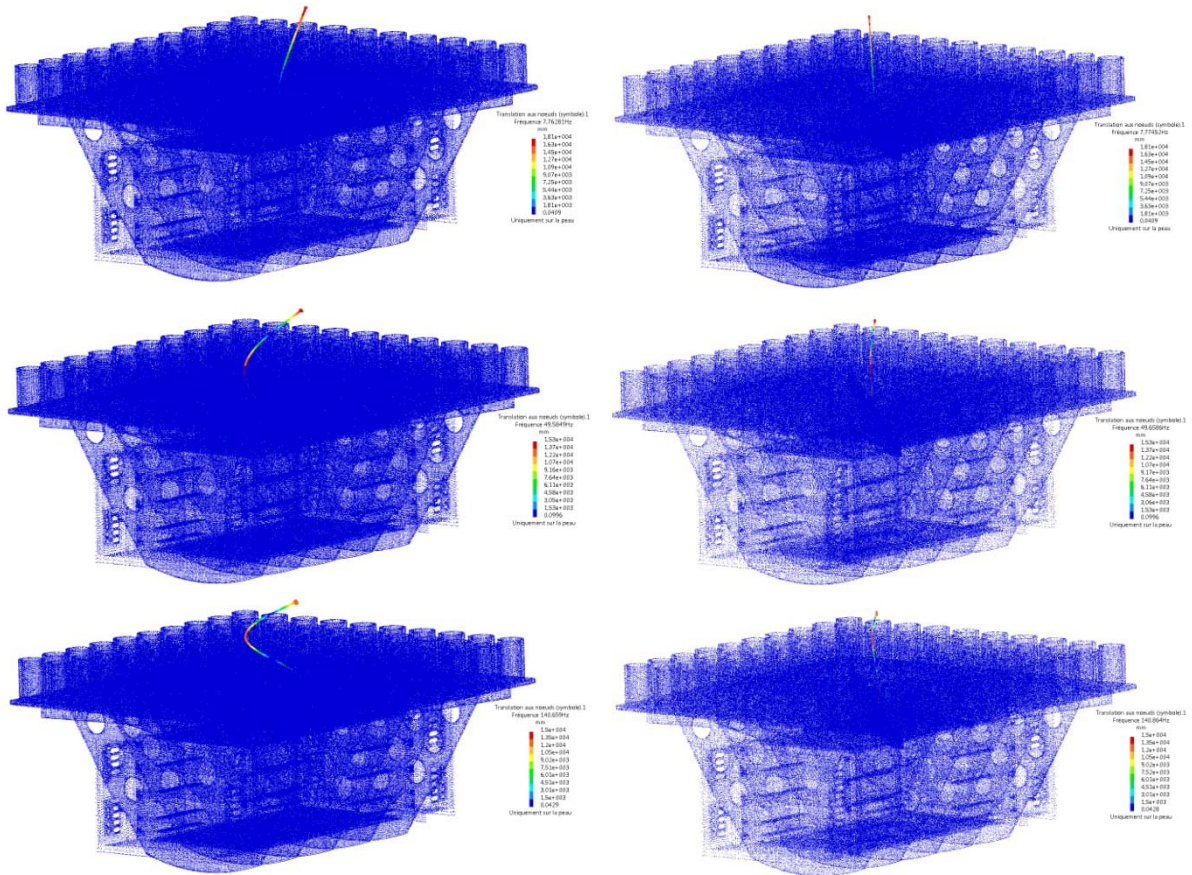
### 6.4.1 Mode 1 to 6: global motion of the bench

The following figures are showing the displacements for the first 6 modes which are just global motions of the bench



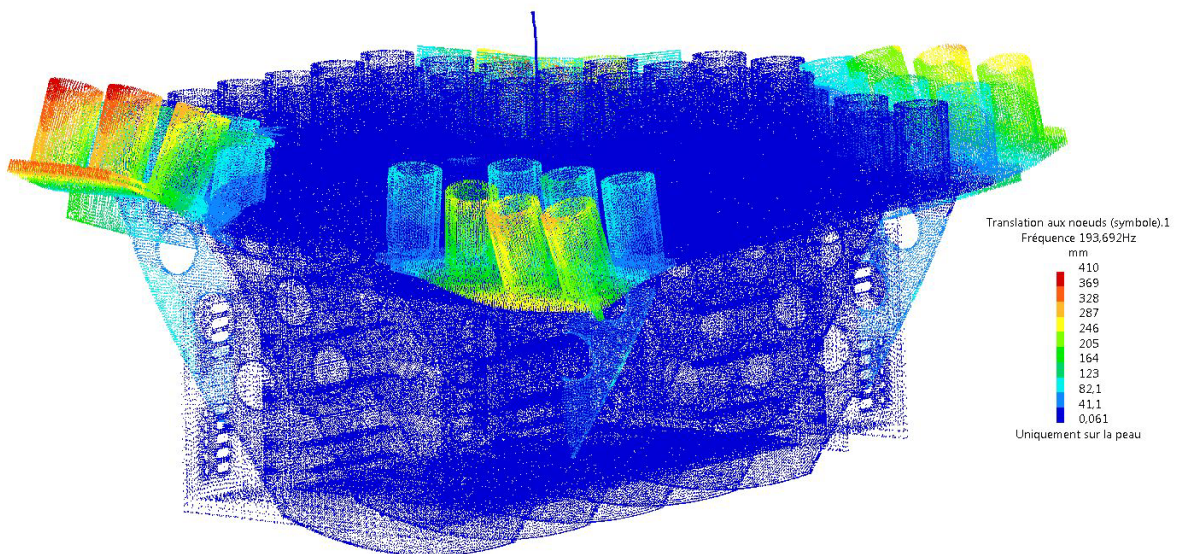
### 6.4.2 Mode 7 to 12: motions of the wire

The following figures are showing the displacements for the next 6 modes (7.76 Hz to 140.86 Hz)



### 6.4.3 First internal mode of the bench: 193 Hz

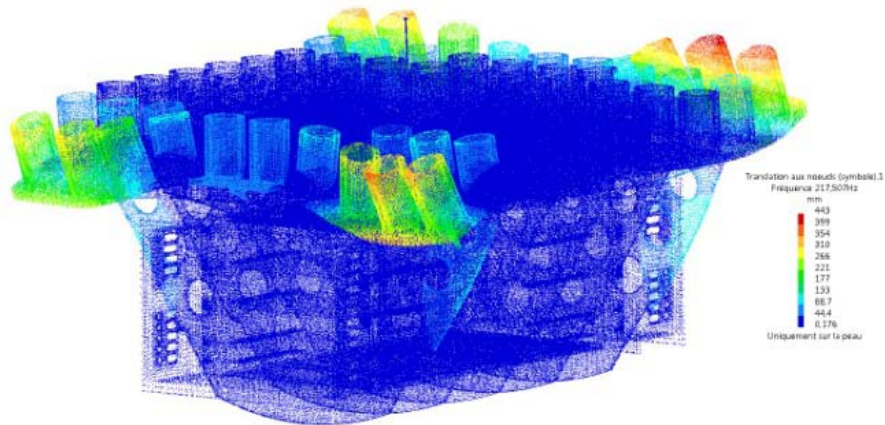
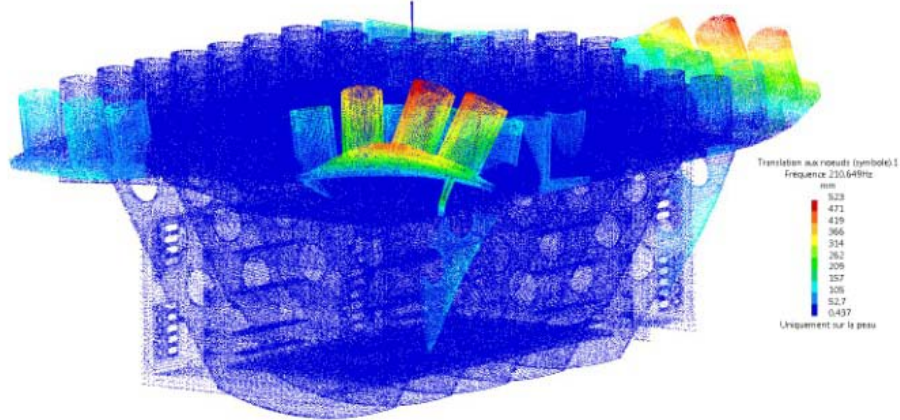
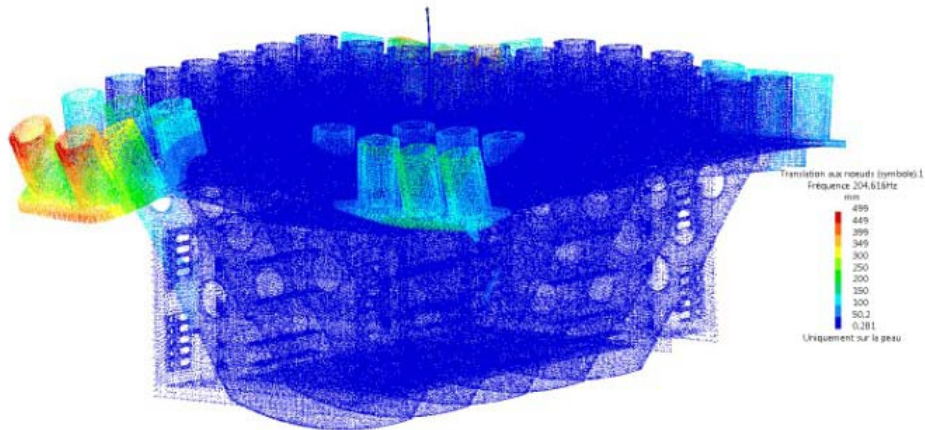
This is the first internal mode of the bench. Its frequency will depend on the final load of each corner of the bench.



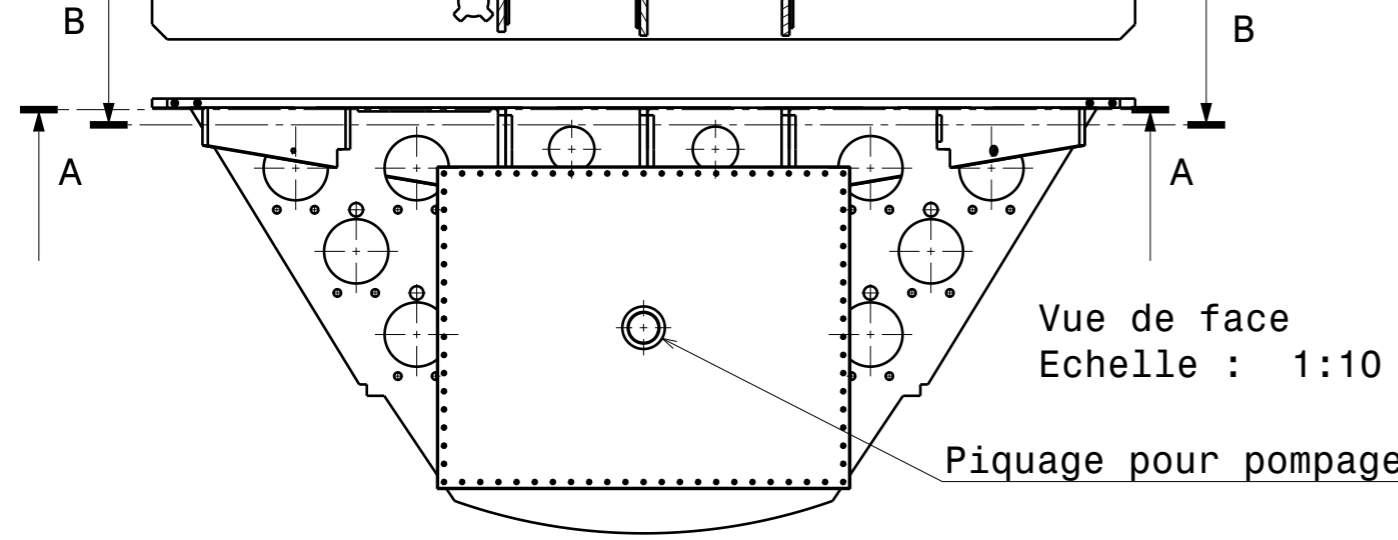
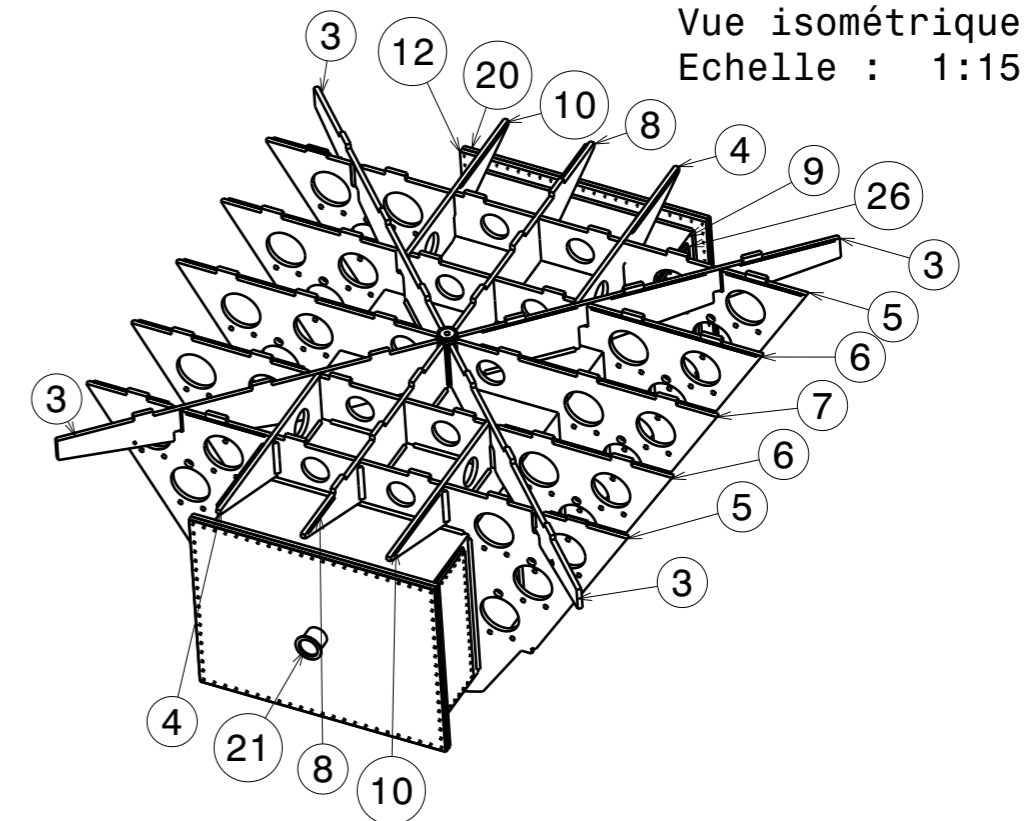
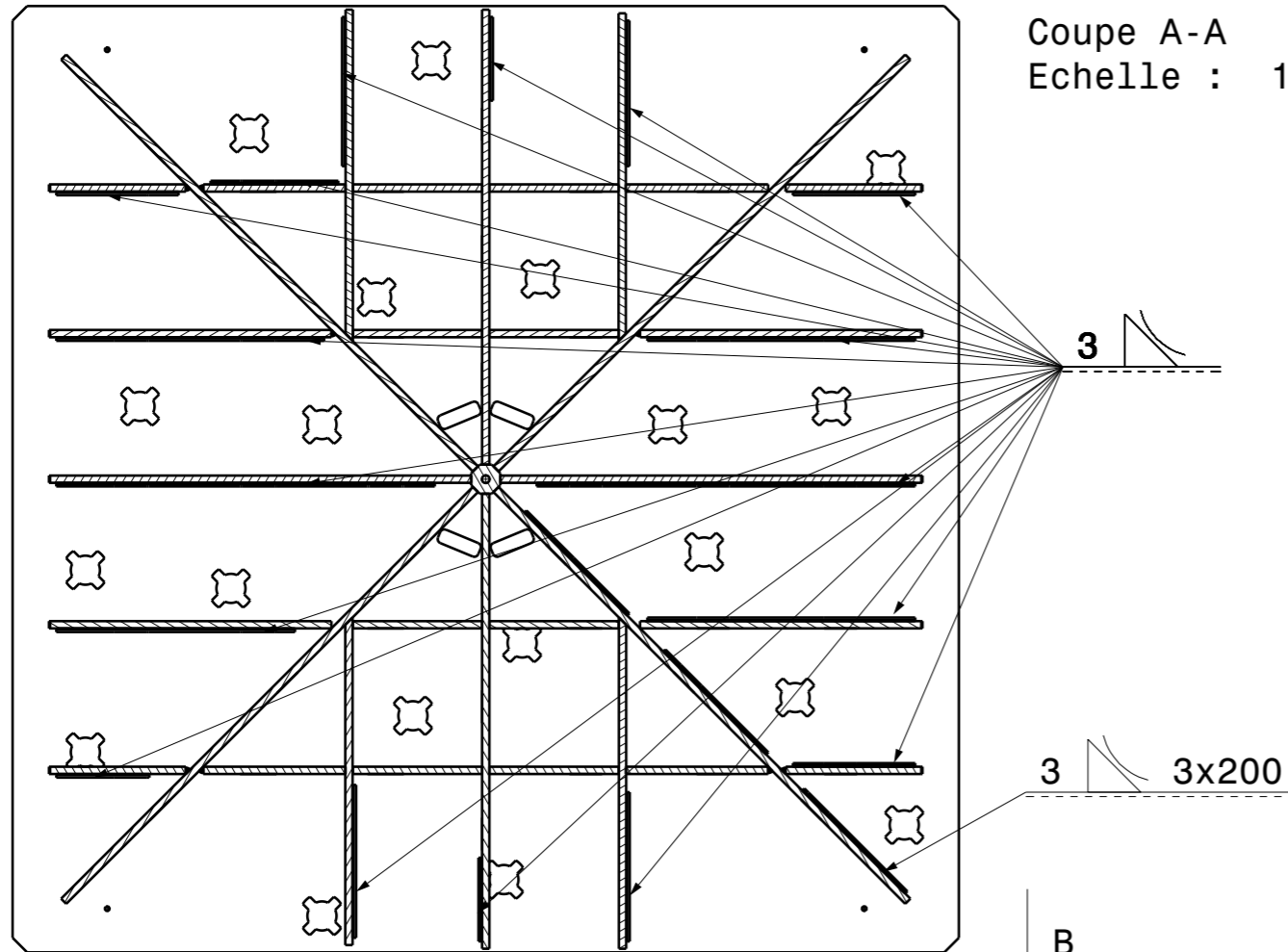


#### 6.4.4 Next 3 modes: 204 to 210Hz

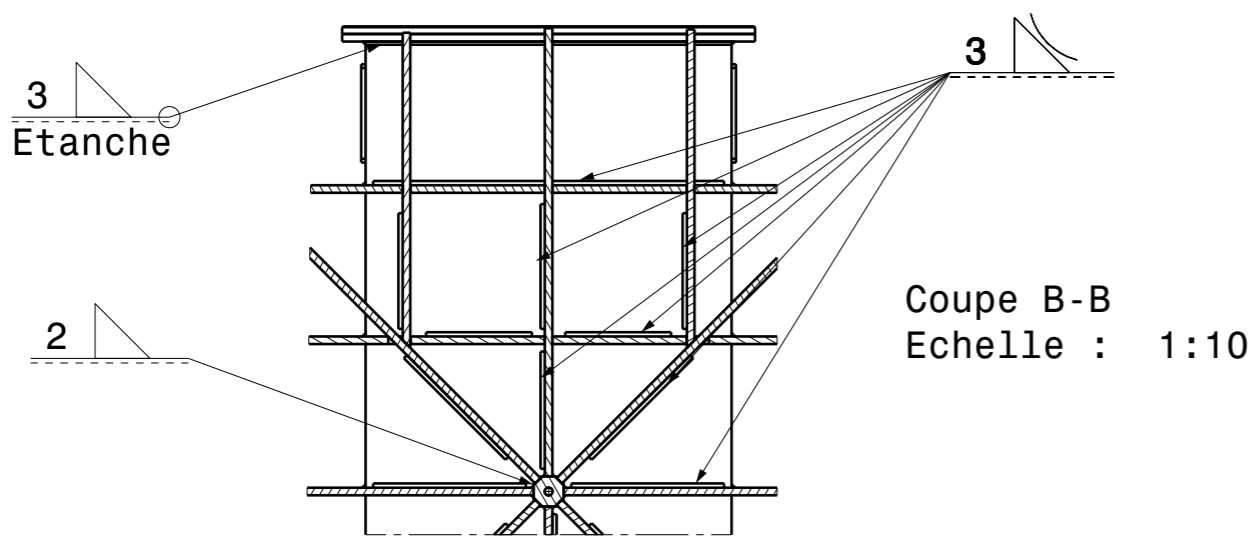
These are other modes due to the motion of the bench corners.



## **7 ANNEX: Bench drawings used for the call for tender**

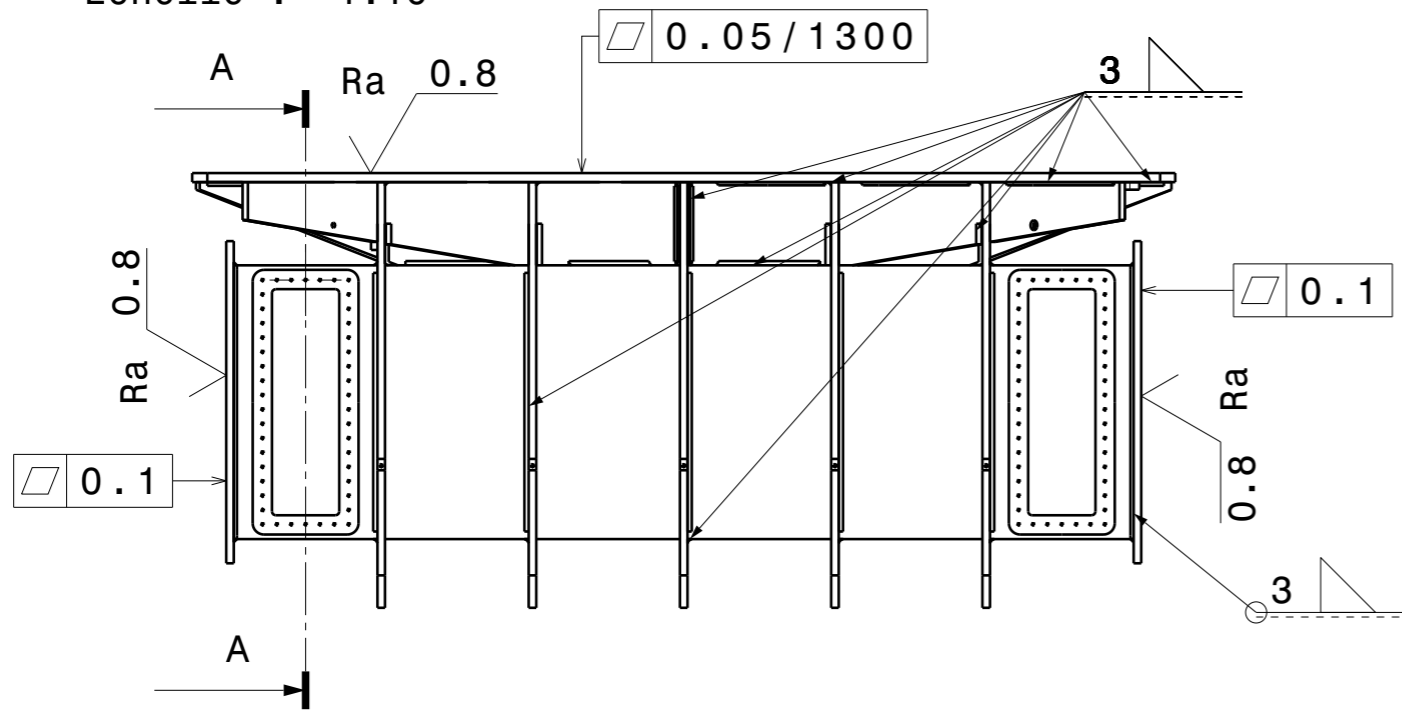


Ref	Nb	Plan	Désignation	SmarTeam	DRW
2	1	064-10-002	Minitour Table Optique	PRT066410	DRW15474
3	4	064-10-003	Minitour Table Optique Nervures Diagonale	PRT066412	DRW15508
4	2	064-10-004	Minitour Table Optique Nervure Axiale ExtG	PRT066413	DRW15521
5	2	064-10-005	Minitour Table Optique Nervure Laterale Ext	PRT066414	DRW15522
6	2	064-10-006	Minitour Table Optique Nervure Laterale Int	PRT066415	DRW15524
7	1	064-10-007	Minitour Table Optique Nervure Laterale Milieu	PRT066416	DRW15526
8	2	064-10-008	Minitour Table Optique Nervure Axiale Milieu	PRT066417	DRW15527
9	1	064-10-009	Minitour Table Optique Tube Electro	PRT066418	DRW15535
10	2	064-10-010	Minitour Table Optique Nervure Axiale ExtD	PRT066419	DRW15536
11	1	064-10-011	Minitour Table Optique Accroche Cable	PRT066420	DRW15537
12	2	064-10-012	MiniTour Collier Rallonge Porte	PRT066429	DRW15538
20	2	064-10-020	Minitour Detecteur Porte	PRT064170	DRW15195
21	1	064-10-021	Minitour Detecteur Porte Pompage	PRT069291	DRW15771
26	4	064-10-026	Connecteur Plaque Pleine	PRT069078	DRW15705

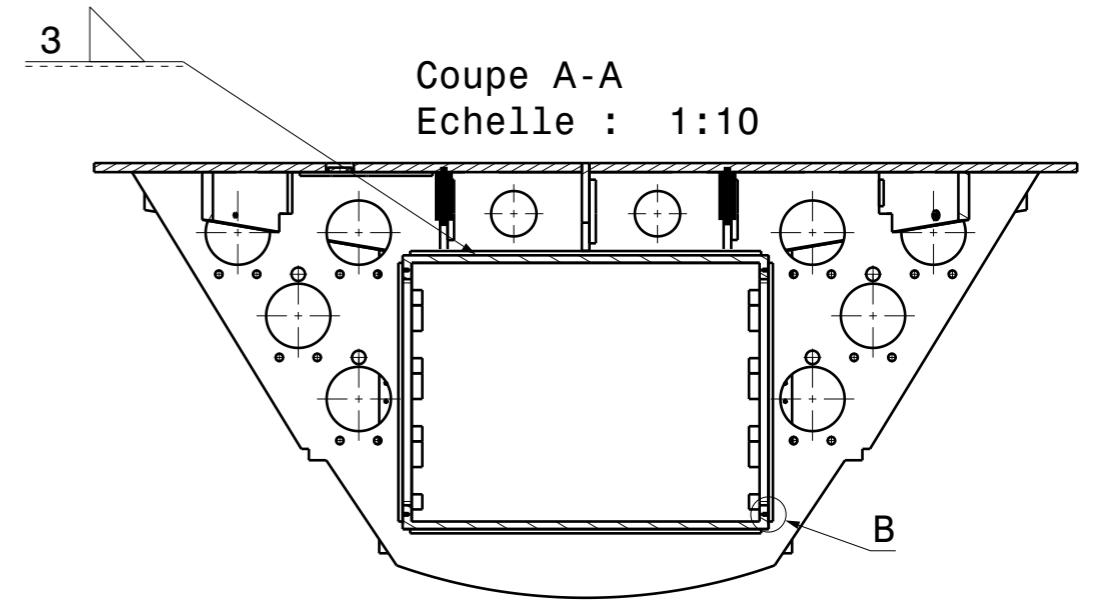


Modification		Author	Date	A
Material:	6060	Ra:	6.3	Project: 064 Advanced-VIRGO
Traitement:	/	Tol:	ISO 2768 mK	Experiment: 10 TableOptique
Qty:	5	Mass:	180 Kg	SmarTeam SLD: PRD16760
		Dims:	mm	SmarTeam DRW: DRW15755
		Scale:	1/10	Date: 2014 March 17
Laboratoire d'Anncy-le-vieux de Physique des Particules BP 110, F-74941 Anncy-Le-Vieux CEDEX			nicolas.allemadou@lapp.in2p3.fr Fax +33 4 50 27 94 95 Ph +33 4 50 09 17 87	
<b>PUMA-Minitour Table Optique</b>			<b>064 10 050</b>	<b>-</b>

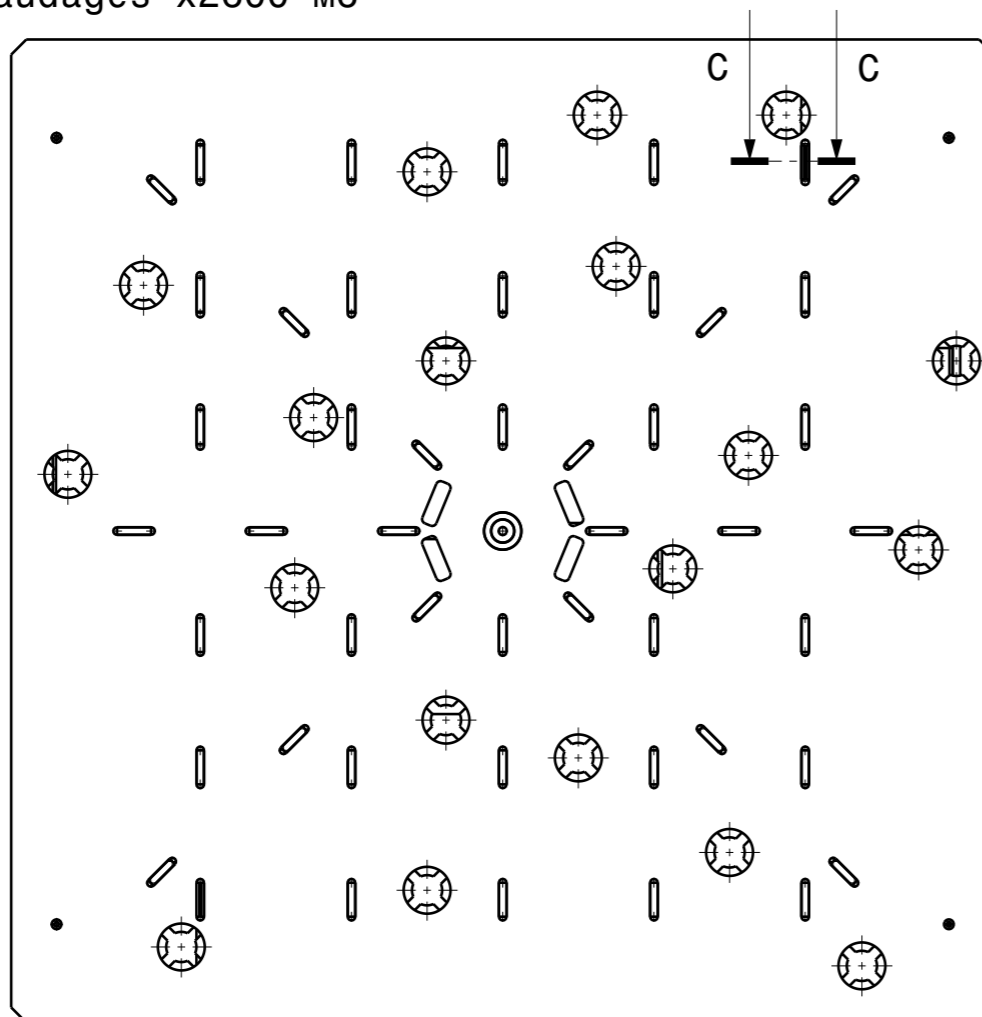
Vue de face  
Echelle : 1:10



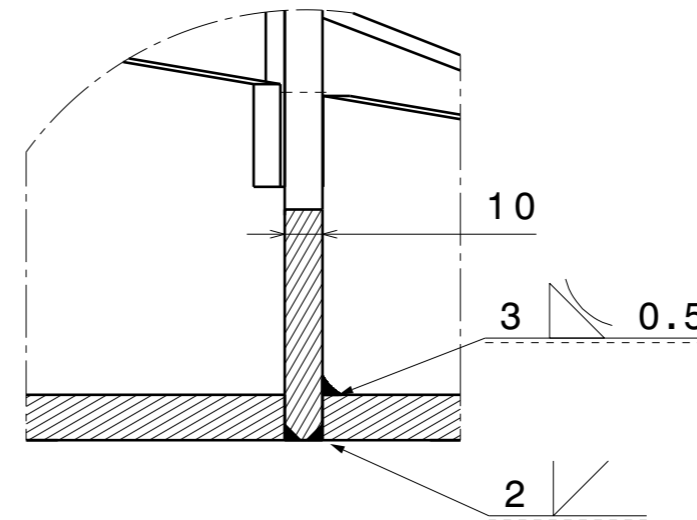
Coupe A-A  
Echelle : 1:10



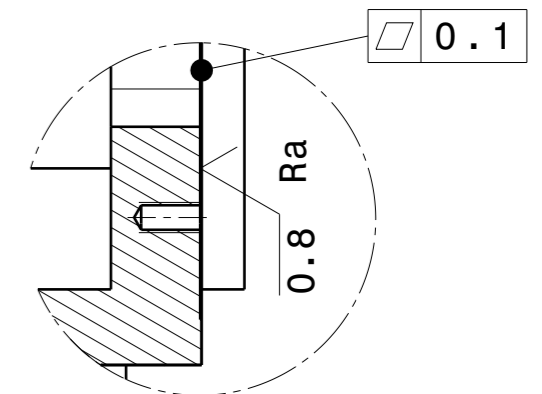
Vue de dessus  
Echelle : 1:10  
+Taraudages x2600 M6



Coupe C-C  
Echelle : 1:2  
Tenon-Mortaise  
Detail soudure



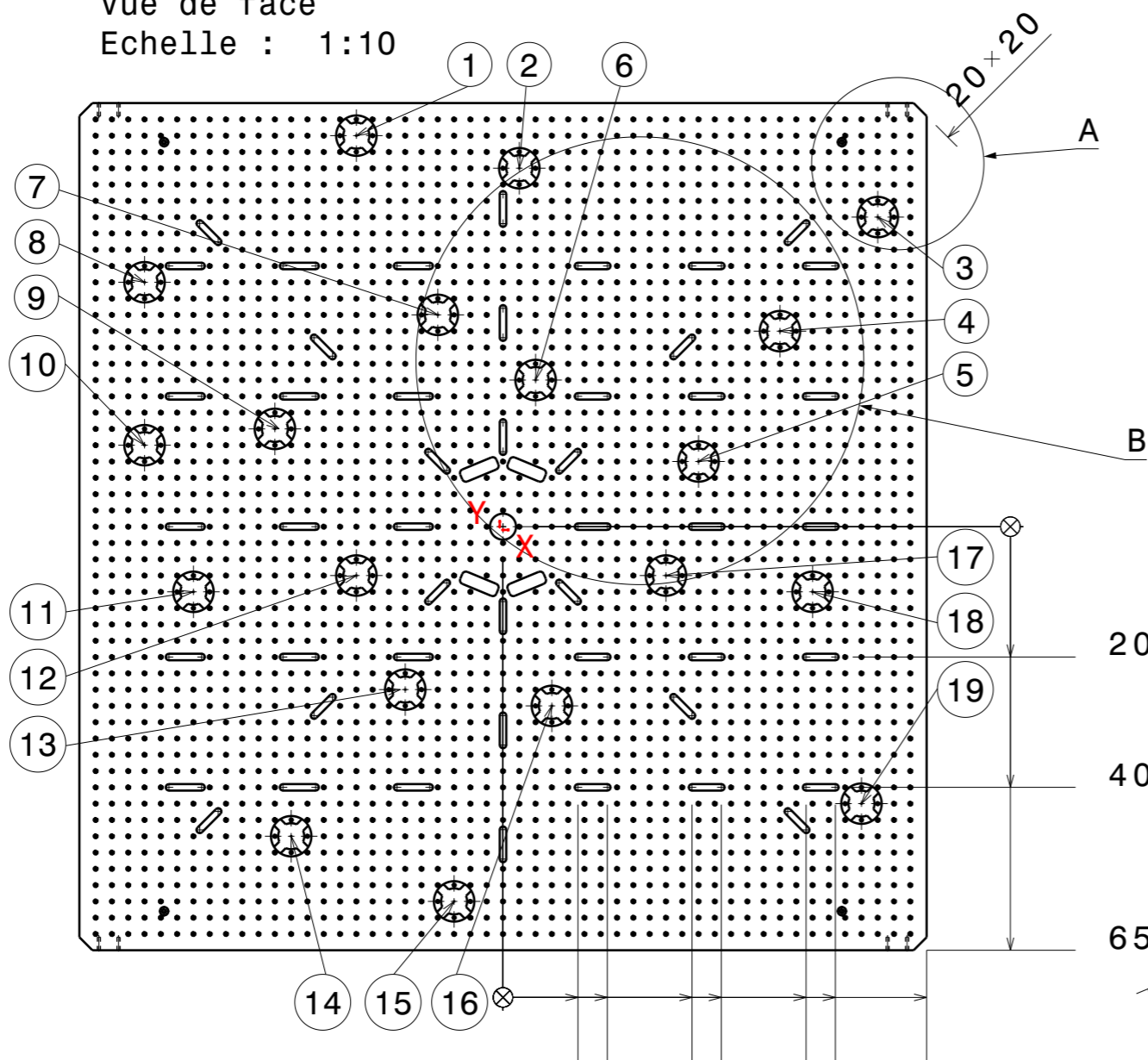
Détail B  
Echelle : 1:1  
Portée de joint x4



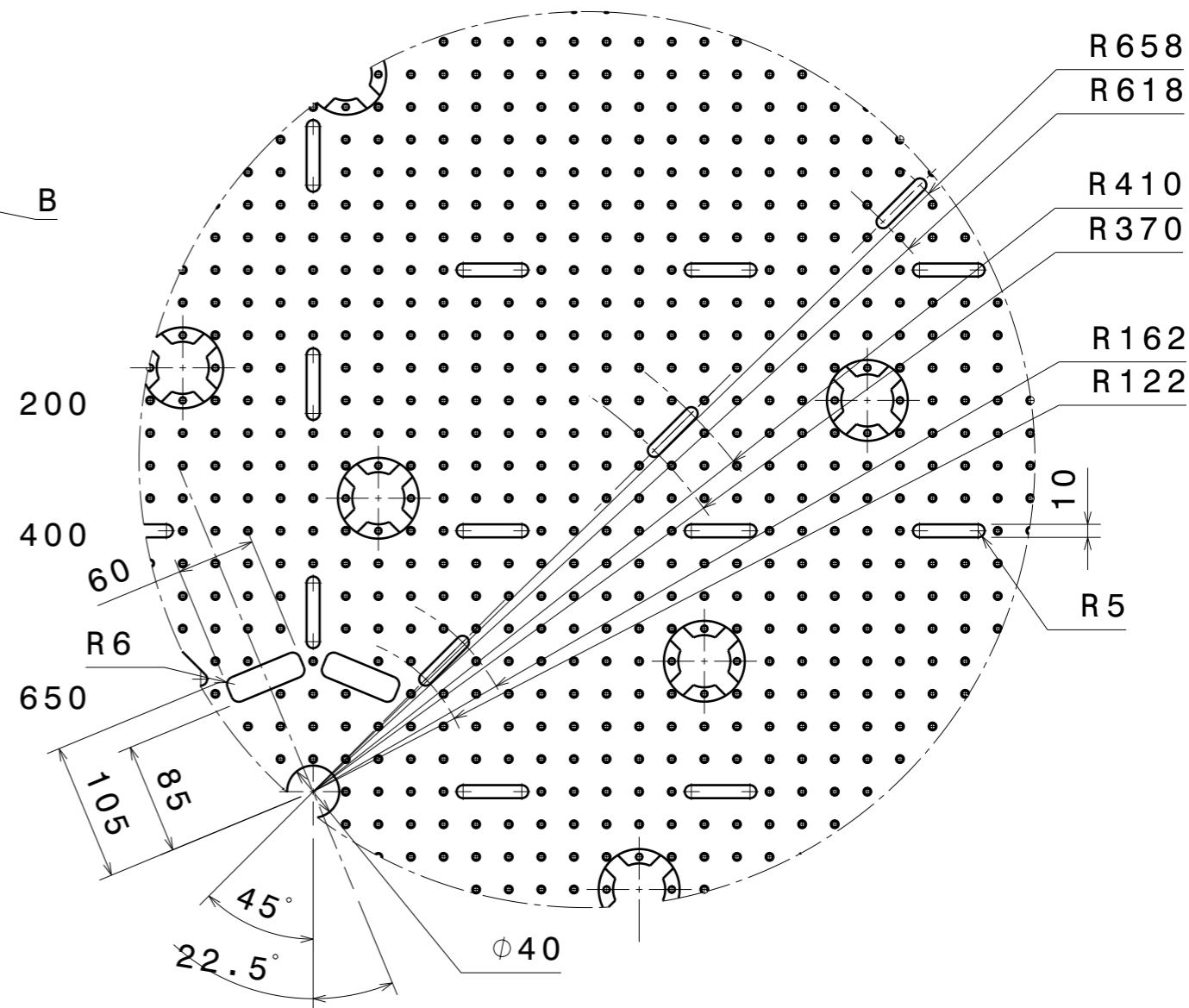
Modification		Author	Date	A
Material:	6060	Ra:	6.3	Project: 064 Advanced-VIRGO
Traitement:	/	Tol:	ISO 2768 mK	Experiment: 10 TableOptique
Qty:	1	Mass:	160 Kg	Smarteam SLD: PRD16148
		Dims:	mm	Smarteam DRW: DRW15553
		Scale:	1/10	Date: 2014 March 17
Laboratoire d'Annecy-le-vieux de Physique des Particules BP 110, F-74941 Annecy-Le-Vieux CEDEX			nicolas.allemadou@lapp.in2p3.fr Fax +33 4 50 27 94 95 Ph +33 4 50 09 17 87	
<b>Assemblage Table Optique</b>			<b>064 10 001</b>	<b>-</b>

REF.	X	Y
1	-225	600
2	25	550
3	575	475
4	425	300
5	300	100
6	50	225
7	-100	325
8	-550	375
9	-350	150
10	-550	125
11	-475	-100
12	-225	-75
13	-150	-250
14	-325	-475
15	-75	-575
16	75	-275
17	250	-75
18	475	-100
19	550	-425

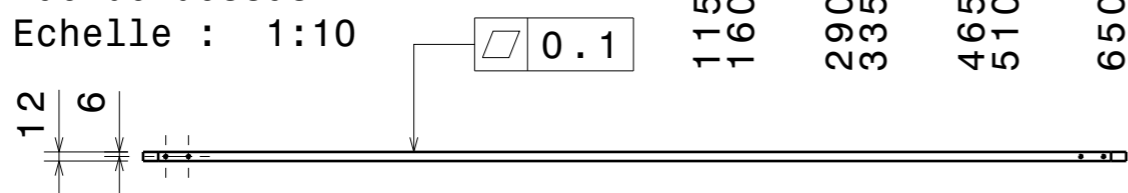
Vue de face  
Echelle : 1:10



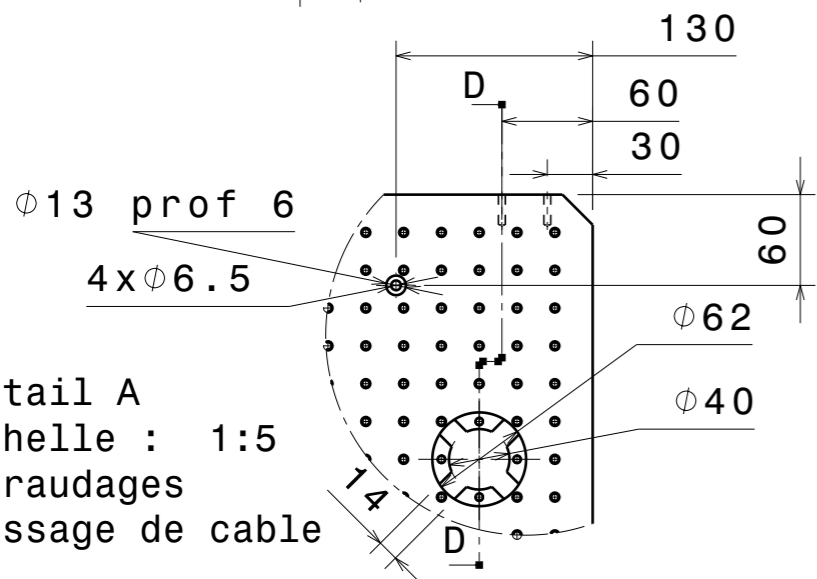
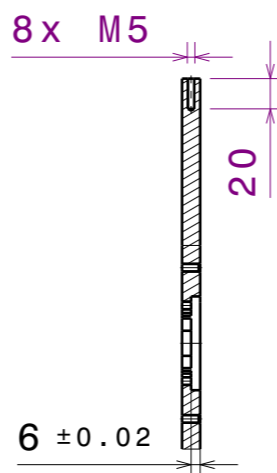
Détail B  
Echelle : 1:5



Vue de dessus  
Echelle : 1:10

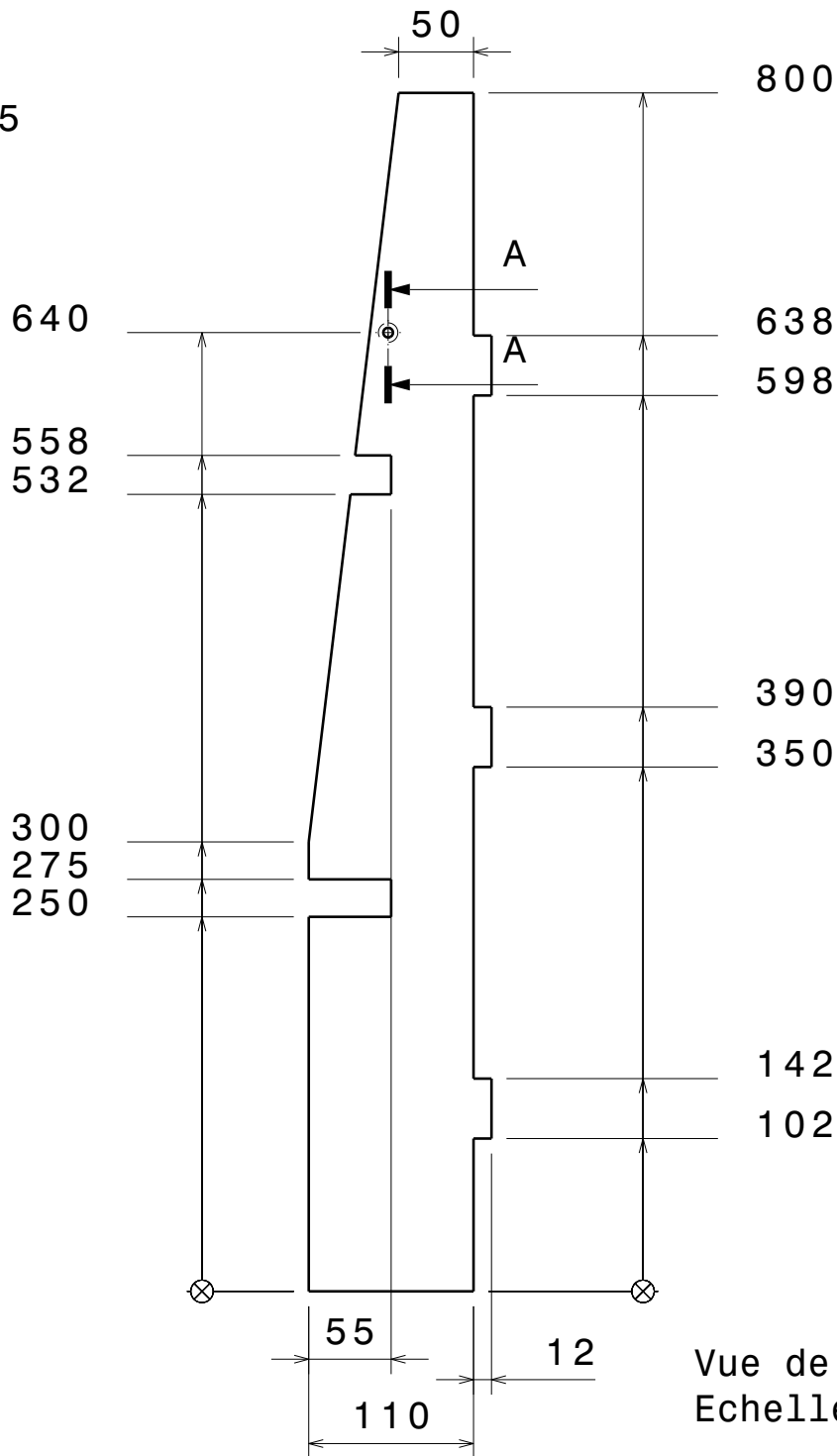
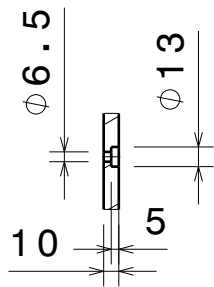


Coupe D-D  
Echelle : 1:5






Modification		Author	Date	A
Material:	6060	Ra:	6.3	Project: 064 Advanced-VIRGO
Traitement:	/	Tol:	ISO 2768 mK	Experiment: 10 TableOptique
Qty:	1	Mass:	50 Kg	Smarteam SLD: PRT066410
		Dims:	mm	Smarteam DRW: DRW15474
		Scale:	1/10	Date: 2014 March 17
Laboratoire d'Anney-le-vieux de Physique des Particules BP 110, F-74941 Anney-Le-Vieux CEDEX		nicolas.allemadou@lapp.in2p3.fr Fax +33 4 50 27 94 95 Ph +33 4 50 09 17 87		
<b>Table Optique</b>			<b>064 10 002</b>	<b>-</b>

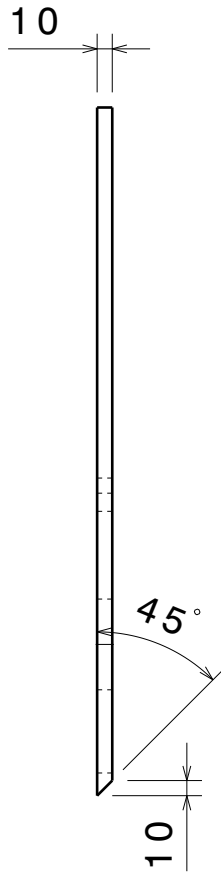
Coupe A-A  
Echelle : 1:5



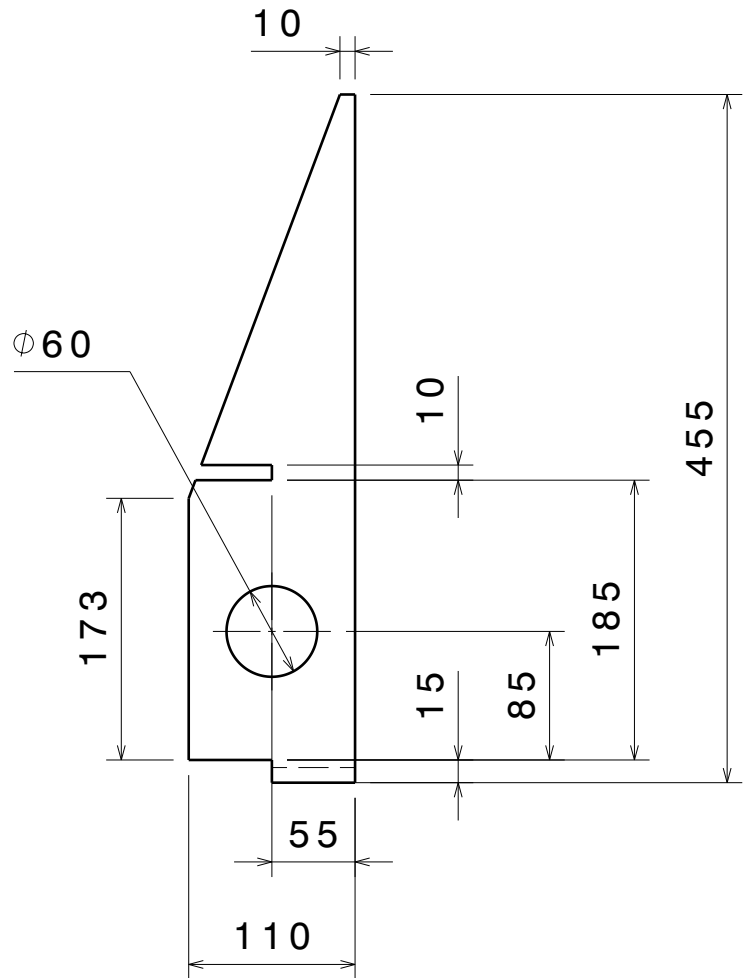
Vue de face  
Echelle : 1:5

Modification		Author	Date	A
Material:	6060	Ra:	3.2	Project: 064 Advanced-VIRGO
Traitement:	/	Tol:	ISO 2768 mK	Experiment: 10 TableOptique
Qty:	4	Mass:	2 Kg	Smarteam SLD: PRT066412
		Dims:	mm	Smarteam DRW: DRW15508
	Scale:	1/5	Date:	2014 March 17
Laboratoire d'Annecy-le-vieux de Physique des Particules BP 110, F-74941 Annecy-Le-Vieux CEDEX		nicolas.allemadou@lapp.in2p3.fr Fax +33 4 50 27 94 95 Ph +33 4 50 09 17 87		
<b>Nervure Diagonale</b>		<b>064 10 003</b>		<b>-</b>

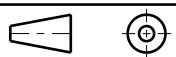
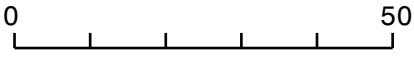


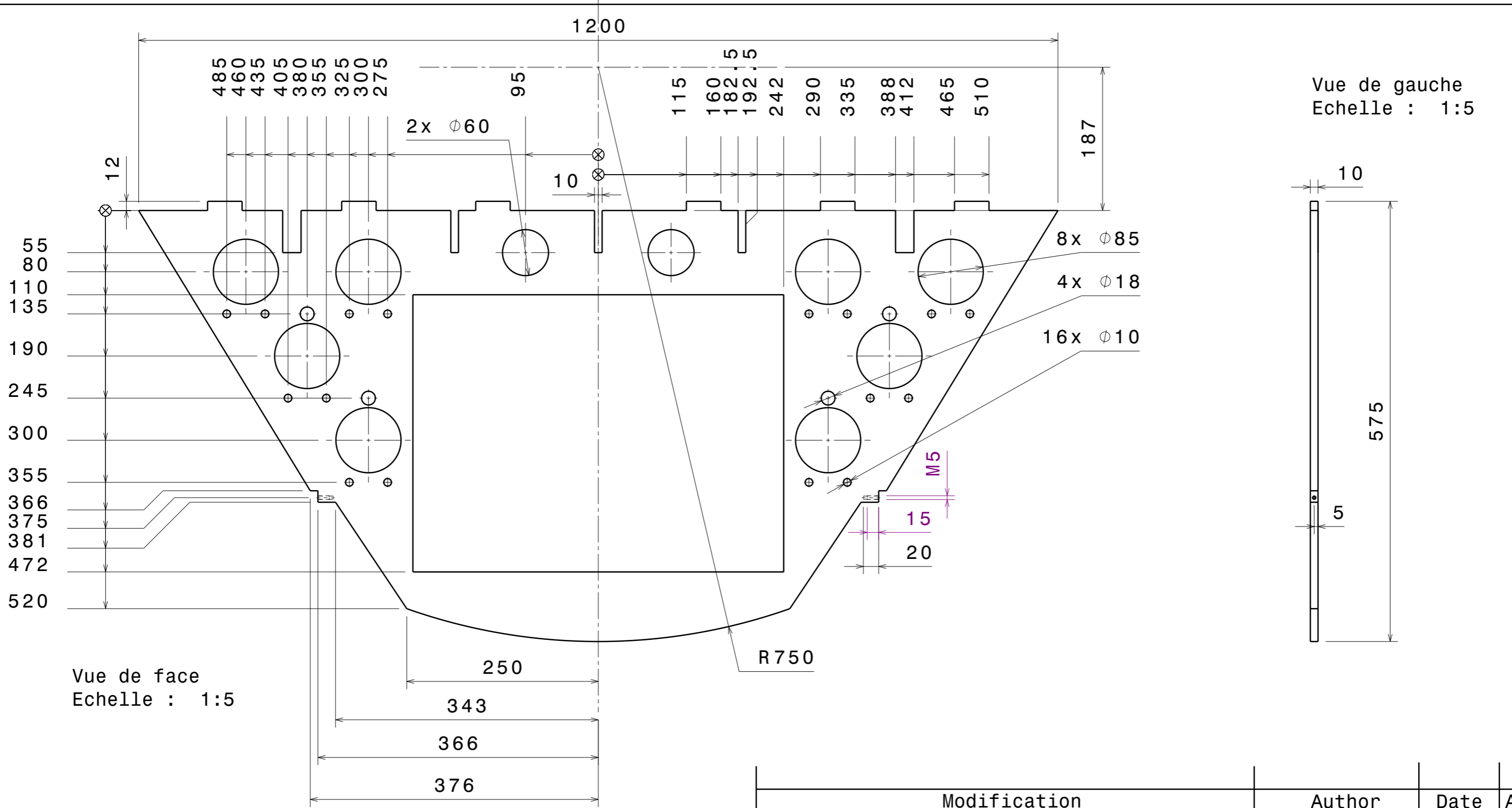


Vue de droite  
Echelle : 1:5



Vue de face  
Echelle : 1:5

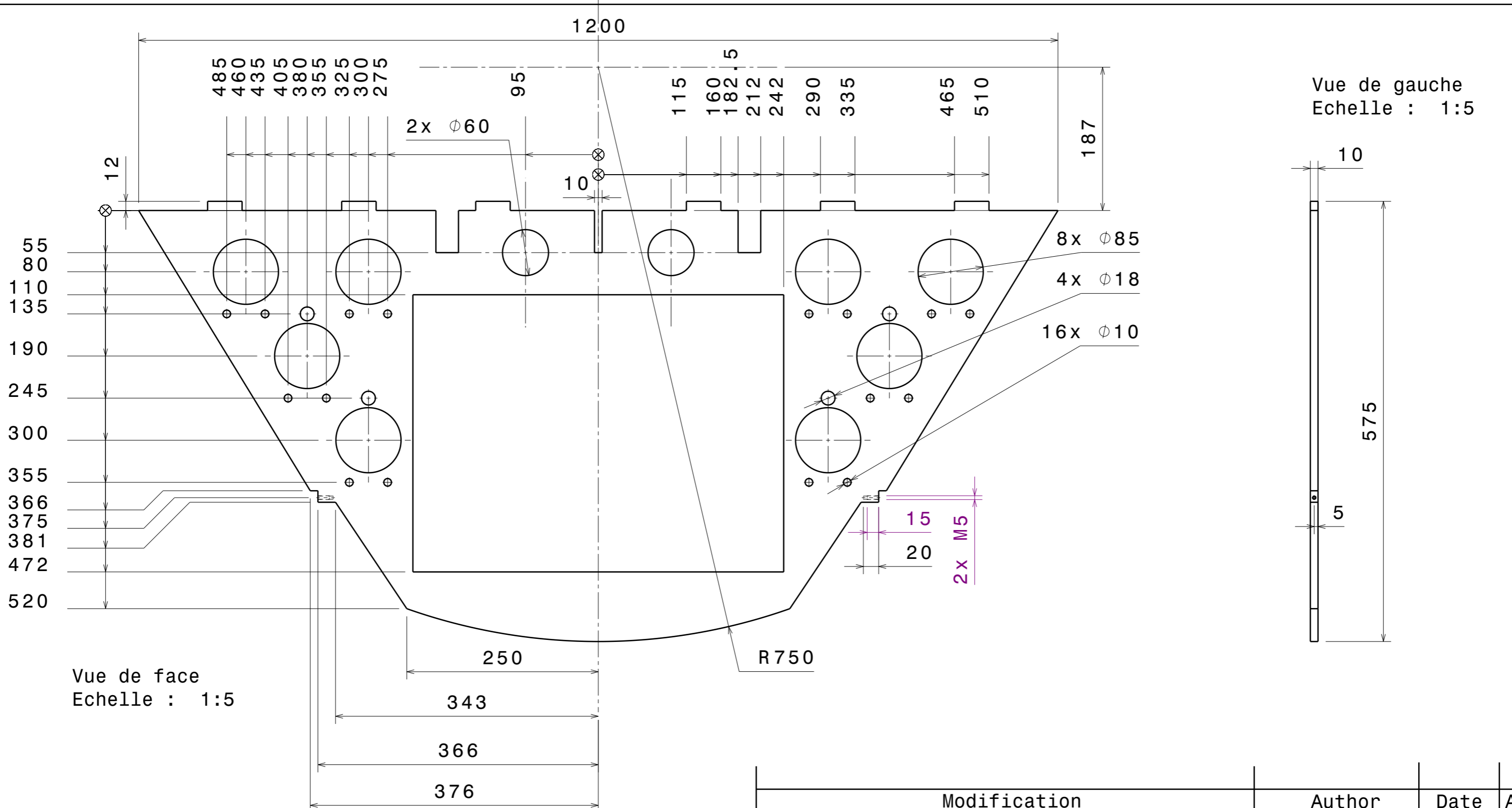
Modification		Author	Date	A
Material:	6060	Ra:	3.2	Project: 064 Advanced-VIRGO
Traitement:	/	Tol:	ISO 2768 mK	Experiment: 10 TableOptique
Qty:	2	Mass:	0.9 Kg	Smarteam SLD: PRT066413
		Dims:	mm	Smarteam DRW: DRW15521
		Scale:	1/5	Date: 2014 March 17
Laboratoire d'Annecy-le-vieux de Physique des Particules BP 110, F-74941 Annecy-Le-Vieux CEDEX		nicolas.allemandou@lapp.in2p3.fr Fax +33 4 50 27 94 95 Ph +33 4 50 09 17 87		
<b>Nervure Axiale Ext G</b>		<b>064 10 004</b>		<b>-</b>

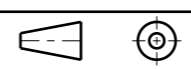



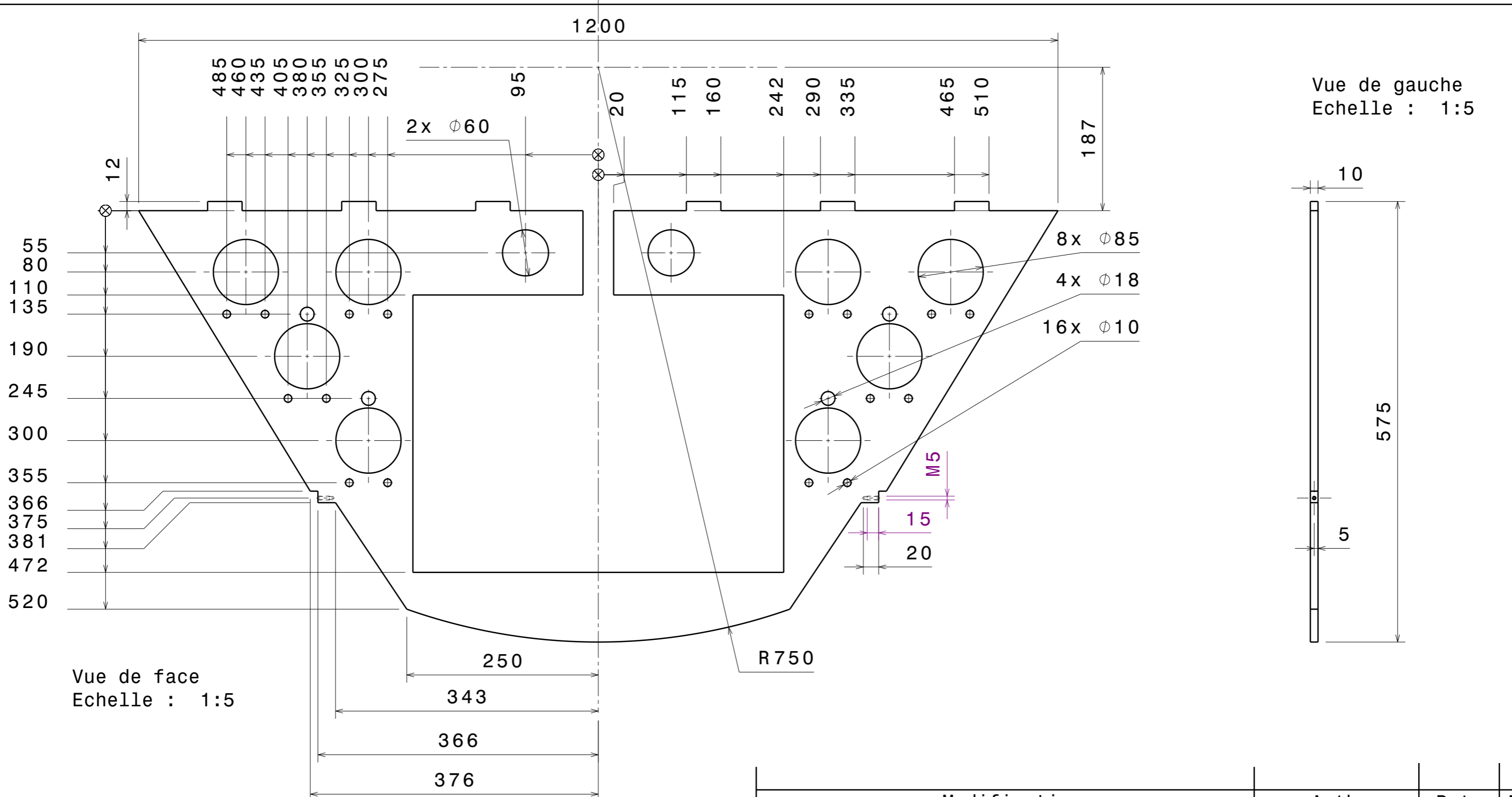
Vue de face  
Echelle : 1:5

Vue de gauche  
Echelle : 1:5

Modification		Author	Date	A
Material:	6060	Ra:	6.3	Project: 064 Advanced-VIRGO
Traitement:	/	Tol:	ISO 2768 mK	Experiment: 10 TableOptique
Qty:	2	Mass:	6.3 Kg	Smarteam SLD: PRT066414
		Dims:	mm	Smarteam DRW: DRW15522
		Scale:	1/5	Date: 2014 March 17
Laboratoire d'Anncy-le-vieux de Physique des Particules BP 110, F-74941 Anncy-Le-Vieux CEDEX		nicolas.allemadou@lapp.in2p3.fr Fax +33 4 50 27 94 95 Ph +33 4 50 09 17 87		
<b>Nervure Laterale Ext</b>		<b>064 10 005</b>		-

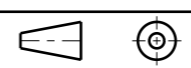



Modification		Author	Date	A	
Material:	6060	Ra:	6.3	Project:	064 Advanced-VIRGO
Traitement:	/	Tol:	ISO 2768 mK	Experiment:	10 TableOptique
Qty:	2	Mass:	6.3 Kg	Smarteam SLD:	PRT066415
		Dims:	mm	Smarteam DRW:	DRW15524
		Scale:	1/5	Date:	2014 March 17
Laboratoire d'Anncy-le-vieux de Physique des Particules BP 110, F-74941 Anncy-Le-Vieux CEDEX				nicolas.allemadou@lapp.in2p3.fr Fax +33 4 50 27 94 95 Ph +33 4 50 09 17 87	
<b>Nervure Laterale Int</b>			<b>064 10 006</b>	<b>-</b>	

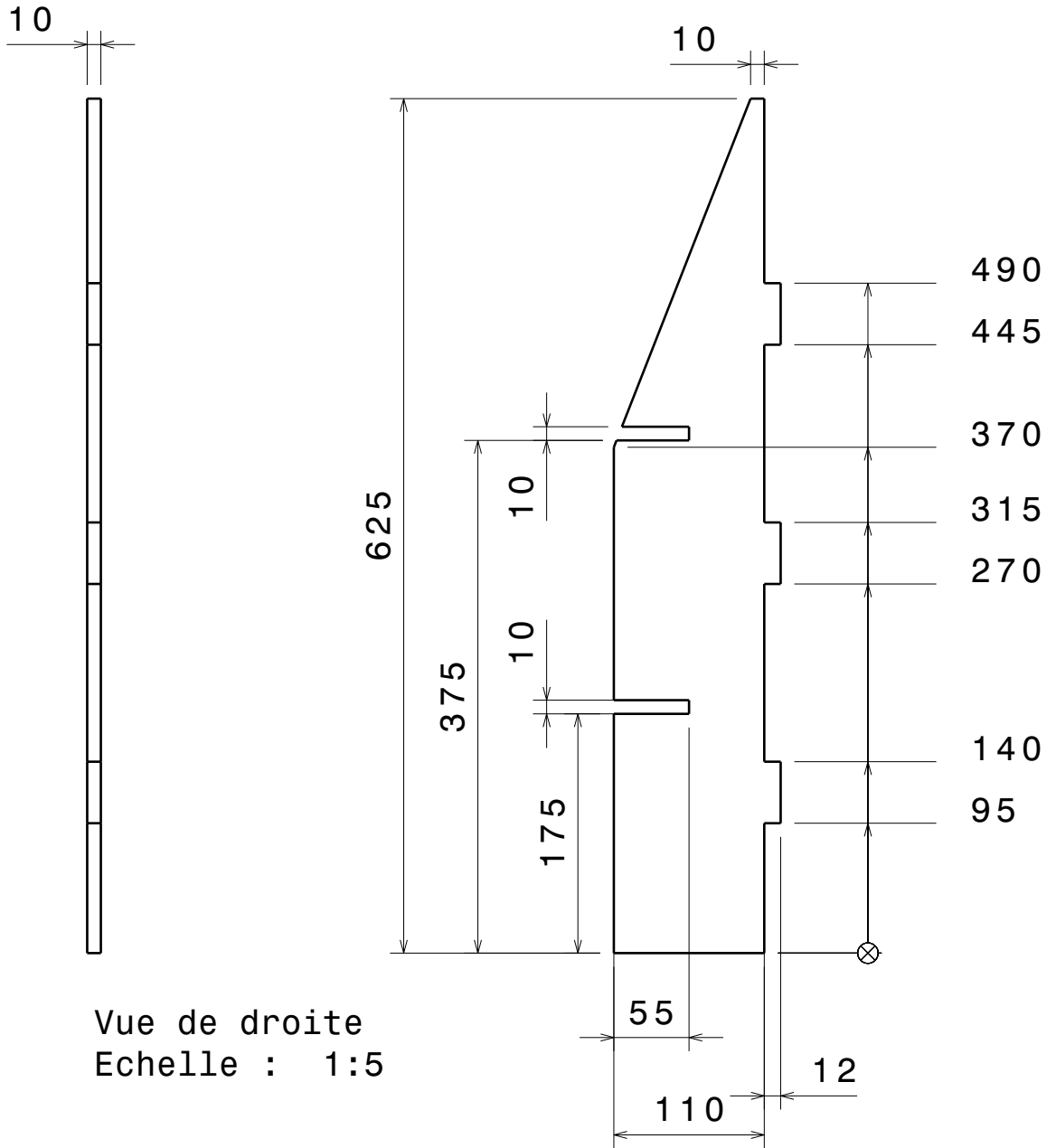


Vue de face  
Echelle : 1:5

Vue de gauche  
Echelle : 1:5

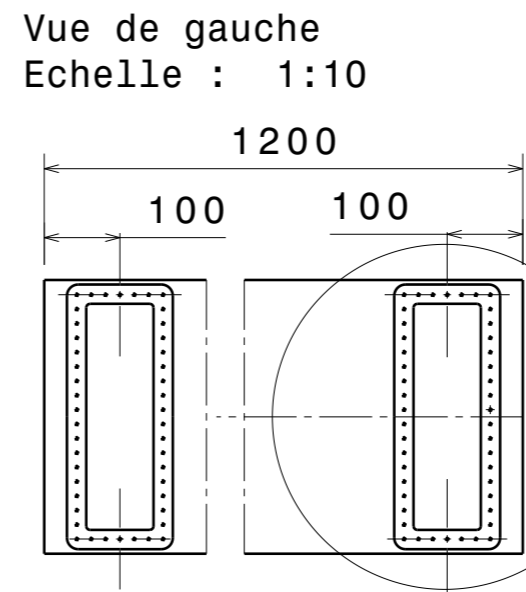
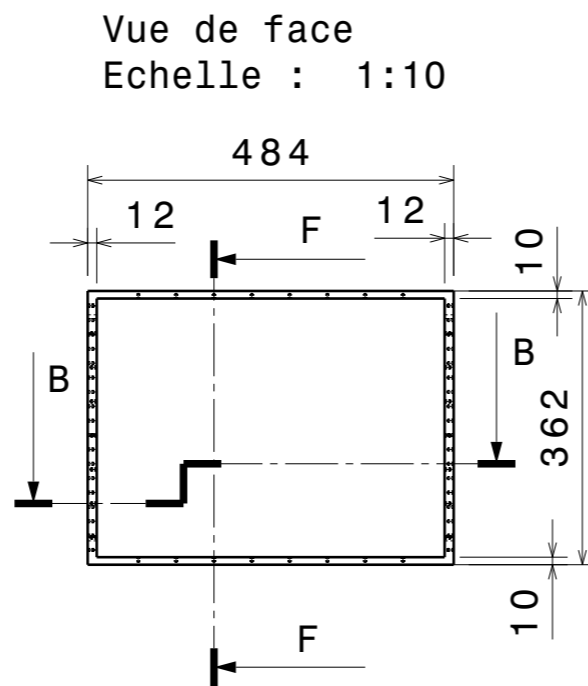
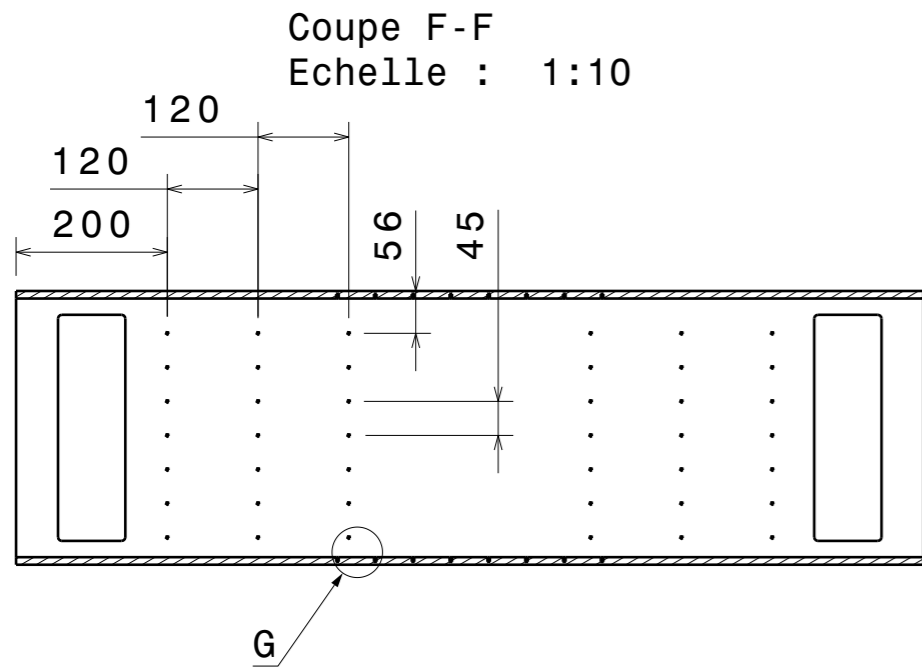
Modification		Author	Date	A	
Material:	6060	Ra:	6.3	Project:	064 Advanced-VIRGO
Traitement:	/	Tol:	ISO 2768 mK	Experiment:	10 TableOptique
Qty:	1	Mass:	6.3 Kg	Smarteam SLD:	PRT066416
		Dims:	mm	Smarteam DRW:	DRW15526
		Scale:	1/5	Date:	2014 March 17
Laboratoire d'Annecy-le-vieux de Physique des Particules BP 110, F-74941 Annecy-Le-Vieux CEDEX				nicolas.allemadou@lapp.in2p3.fr Fax +33 4 50 27 94 95 Ph +33 4 50 09 17 87	
<b>Nervure Laterale Milieu</b>			<b>064 10 007</b>	<b>-</b>	

Vue de face  
Echelle : 1:5

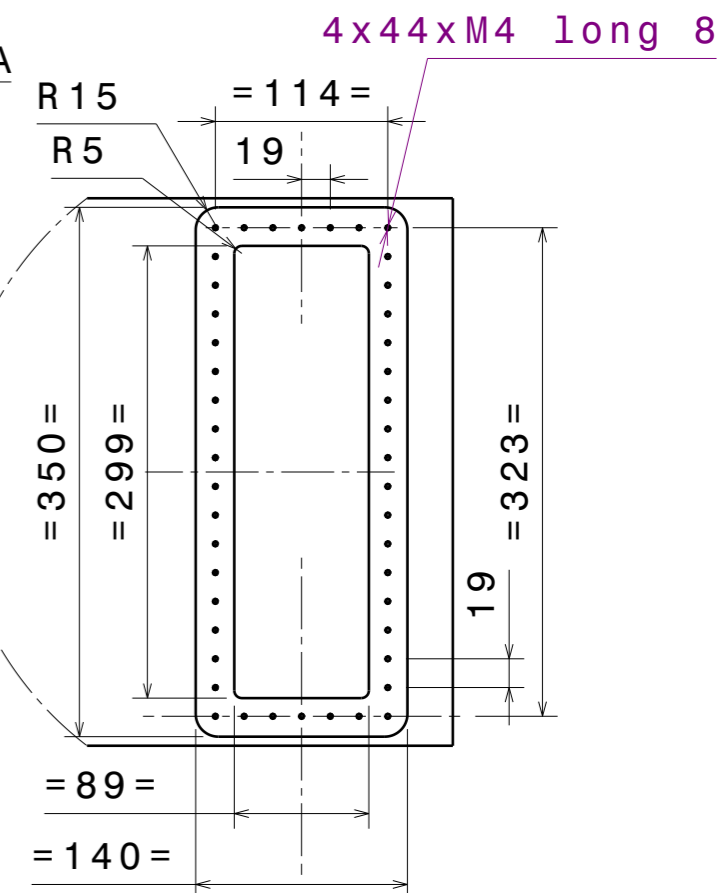


Vue de droite  
Echelle : 1:5

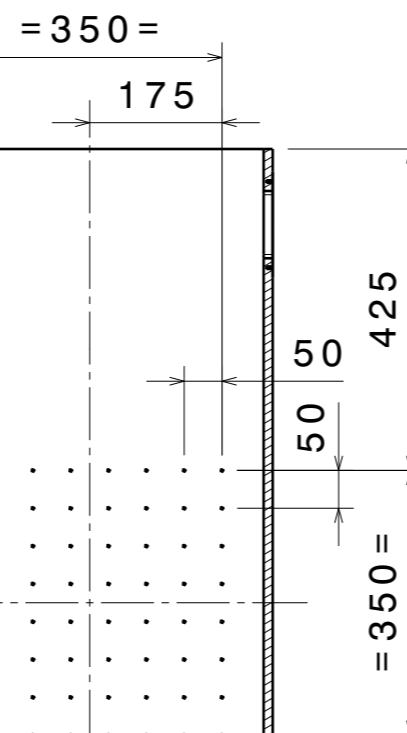
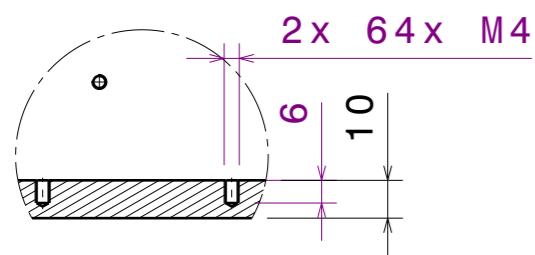
Modification		Author	Date	A
Material:	6060	Ra:	3.2	Project: 064 Advanced-VIRGO
Traitement:	/	Tol:	ISO 2768 mK	Experiment: 10 TableOptique
Qty:	2	Mass:	1.5 Kg	Smarteam SLD: PRT066417
		Dims:	mm	Smarteam DRW: DRW15527
		Scale:	1/5	Date: 2014 March 17
Laboratoire d'Anecy-le-vieux de Physique des Particules BP 110, F-74941 Anecy-Le-Vieux CEDEX		nicolas.allemandou@lapp.in2p3.fr Fax +33 4 50 27 94 95 Ph +33 4 50 09 17 87		
<b>Nervure Axiale Milieu</b>		<b>064 10 008</b>	<b>-</b>	



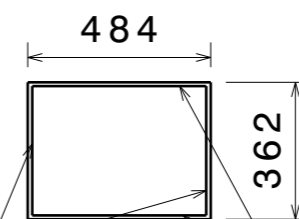
Détail A  
Echelle : 1:5  
4 lumières



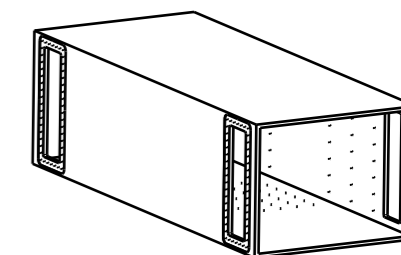
Détail G  
Echelle : 1:2  
Taraudage hauts&bas Interne



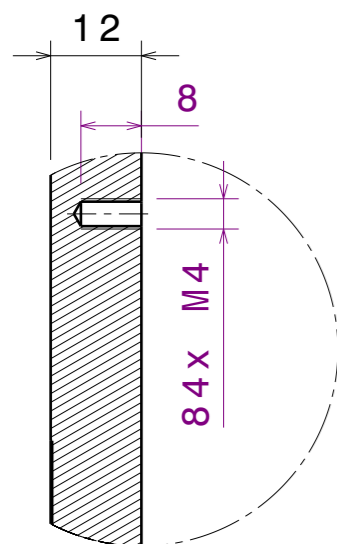
Vue de face  
Echelle : 1:20



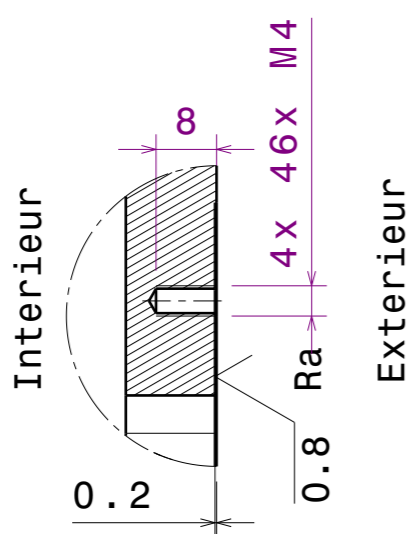
Vue isométrique  
Echelle : 1:20



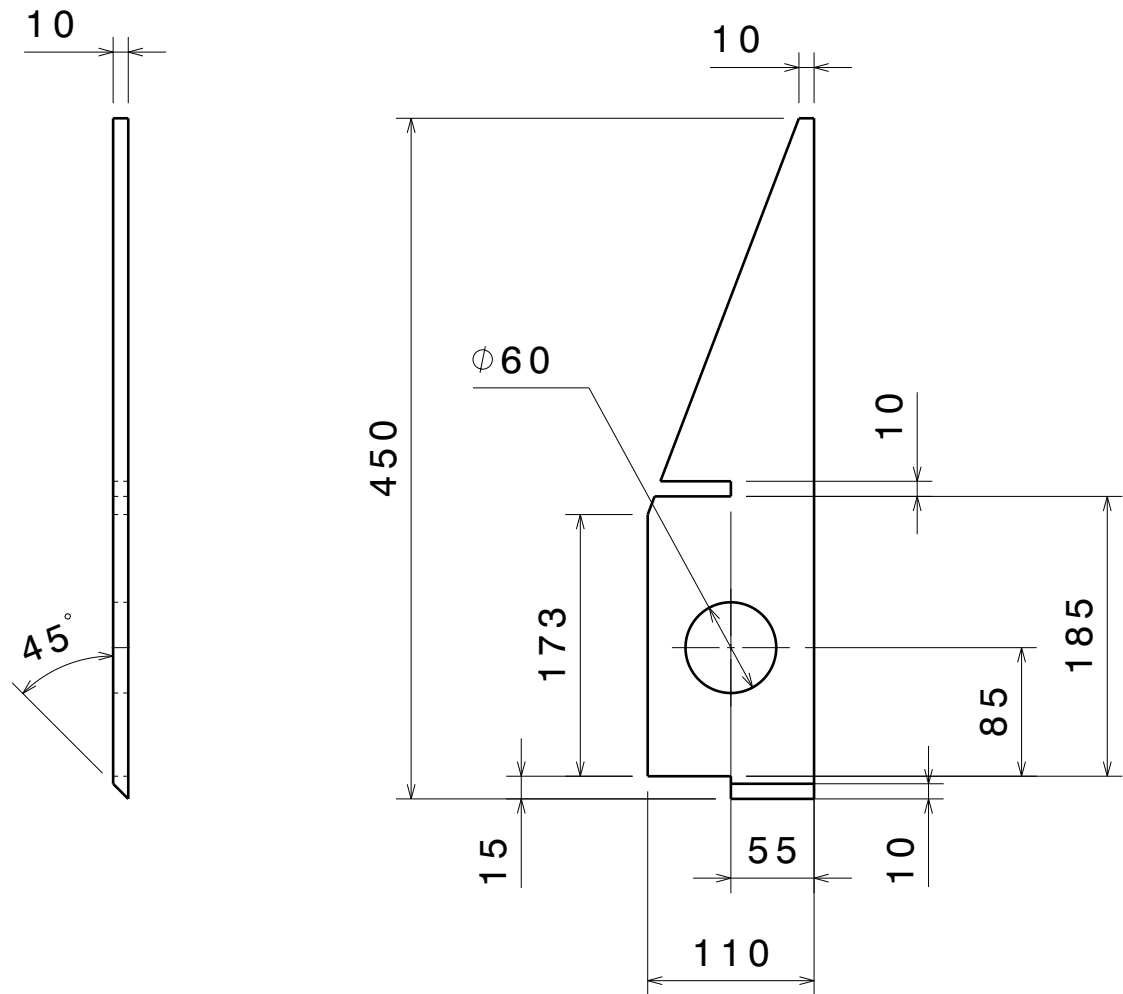
Détail E  
Echelle : 1:1  
Fixation Interne



Détail D  
Echelle : 1:1  
Surfaçage  
Fixation Externe

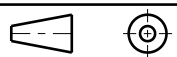
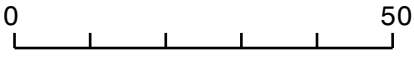


Modification		Author	Date	A
Material:	6060	Ra:	6.3	Project: 064 Advanced-VIRGO
Traitement:	/	Tol:	ISO 2768 mK	Experiment: 10 TableOptique
Qty:	1	Mass:	54 Kg	Smarteam SLD: PRT066418
		Dims:	mm	Smarteam DRW: DRW15535
		Scale:	1/10	Date: 2014 March 17
Laboratoire d'Anney-le-vieux de Physique des Particules BP 110, F-74941 Anney-Le-Vieux CEDEX			nicolas.allemadou@lapp.in2p3.fr Fax +33 4 50 27 94 95 Ph +33 4 50 09 17 87	
<b>Tube Electro</b>			<b>064 10 009</b>	<b>-</b>

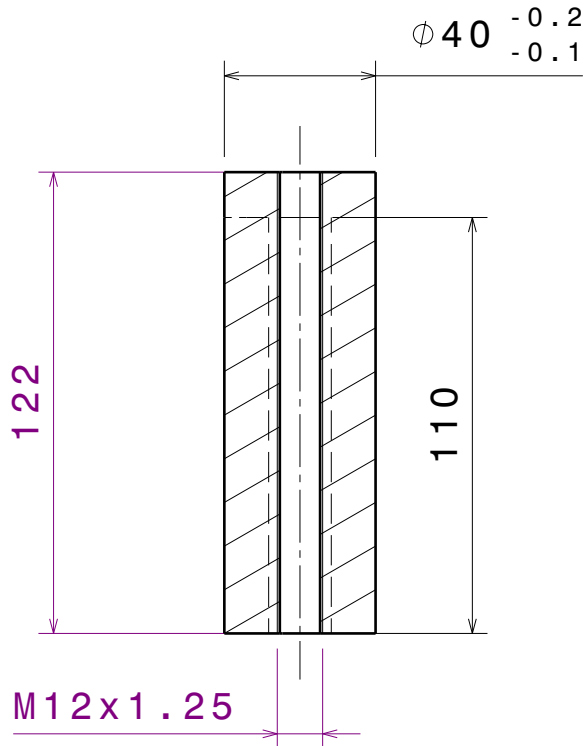


Vue de droite  
Echelle : 1:5

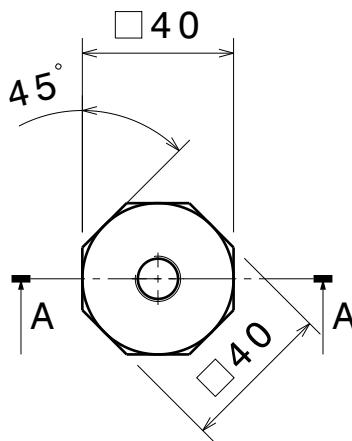
Vue de face  
Echelle : 1:5

Modification		Author	Date	A
Material:	6060	Ra:	3.2	Project: 064 Advanced-VIRGO
Traitement:	/	Tol:	ISO 2768 mK	Experiment: 10 TableOptique
Qty:	2	Mass:	0.9 Kg	Smarteam SLD: PRT066419
		Dims:	mm	Smarteam DRW: DRW15536
		Scale:	1/5	Date: 2014 March 17
Laboratoire d'Annecy-le-vieux de Physique des Particules BP 110, F-74941 Annecy-Le-Vieux CEDEX		nicolas.allemandou@lapp.in2p3.fr Fax +33 4 50 27 94 95 Ph +33 4 50 09 17 87		
<b>Nervure Axiale Ext D</b>		<b>064 10 010</b>		<b>-</b>

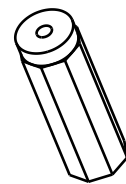
Coupe A-A  
Echelle : 1:2



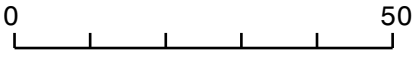


Vue de face  
Echelle : 1:2

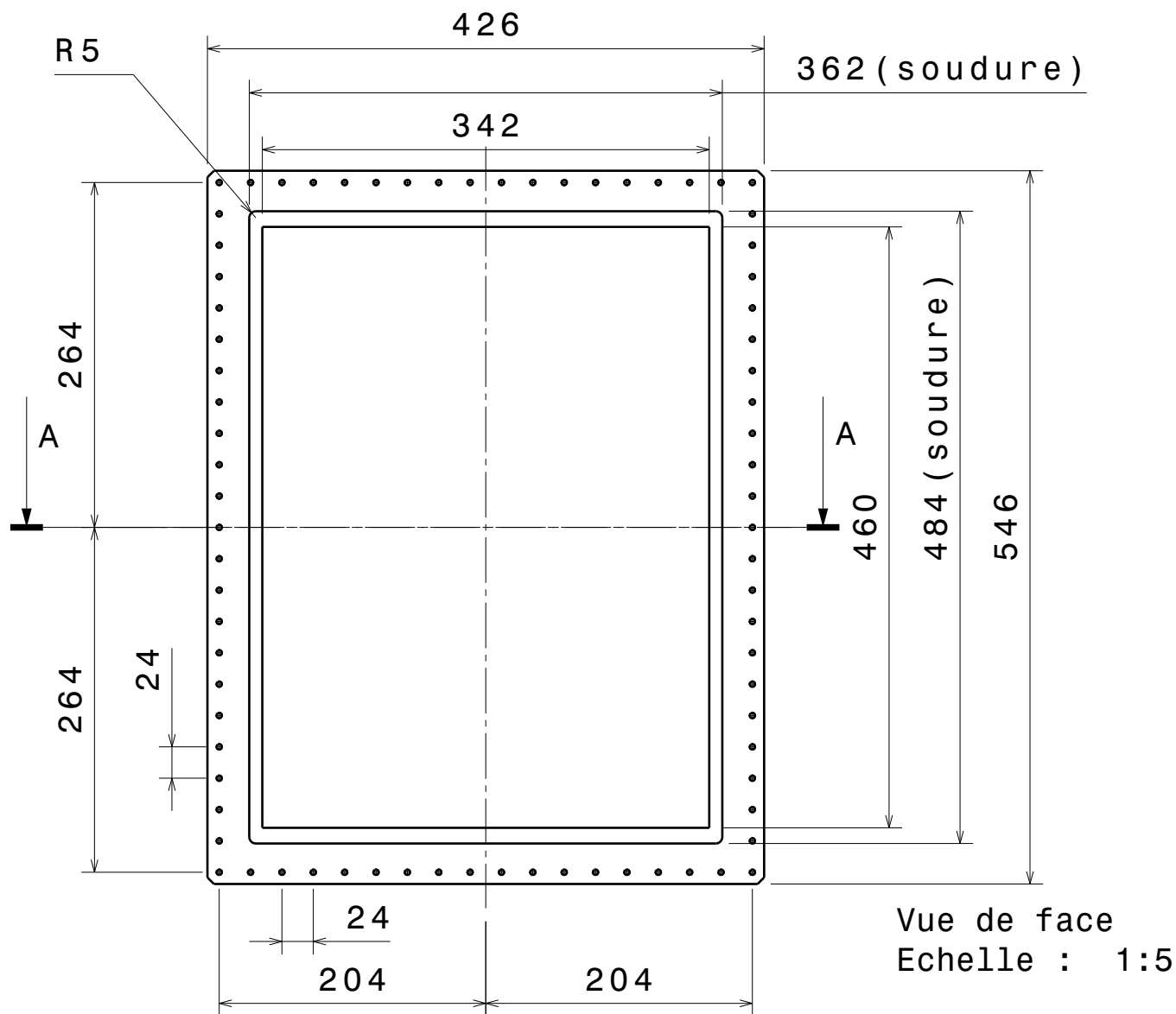


Vue isométrique  
Echelle : 1:5

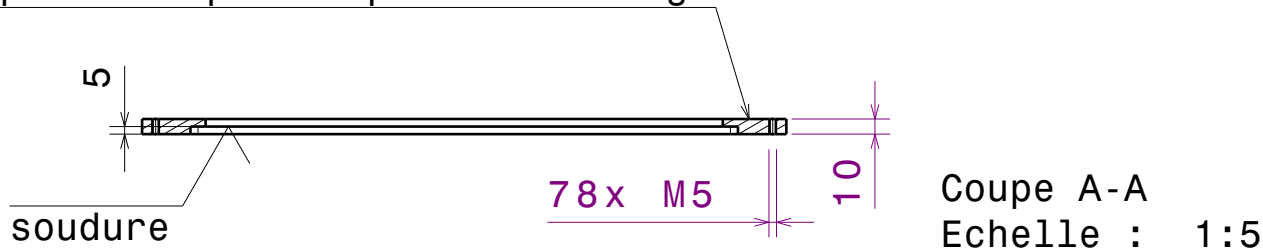


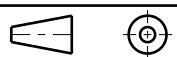

Modification		Author	Date	A
Material:	6060	Ra:	3.2	Project: 064 Advanced-VIRGO
Traitement:	/	Tol:	ISO 2768 mK	Experiment: 10 TableOptique
Qty:	1	Mass:	0.4 Kg	Smarteam SLD: PRT066420
 		Dims:	mm	Smarteam DRW: DRW15537
		Scale:	1/2	Date: 2014 March 17
Laboratoire d'Anecy-le-vieux de Physique des Particules BP 110, F-74941 Anecy-Le-Vieux CEDEX		nicolas.allemadou@lapp.in2p3.fr Fax +33 4 50 27 94 95 Ph +33 4 50 09 17 87		
<b>Accroche cable</b>		<b>064 10 011</b>		<b>-</b>

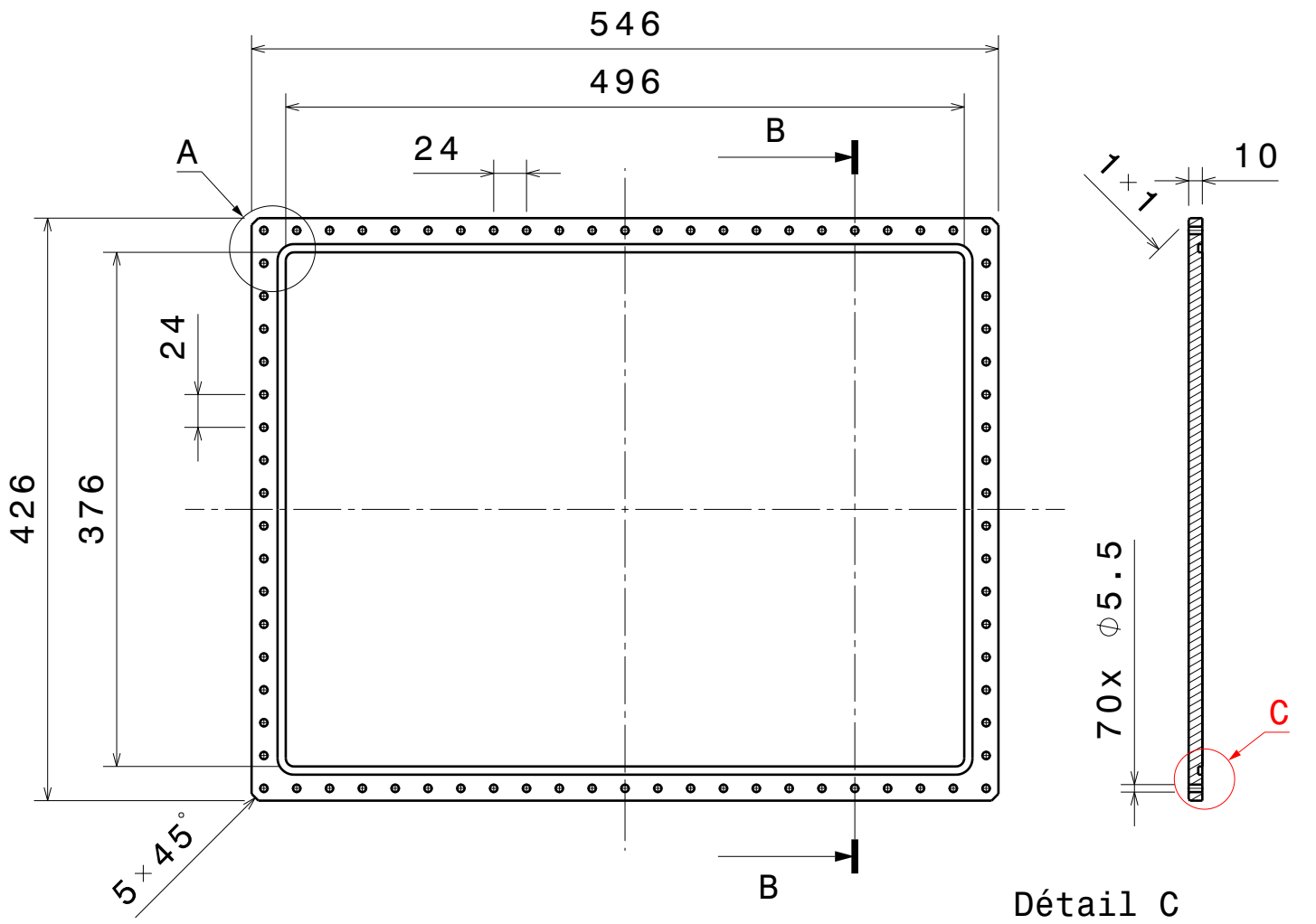




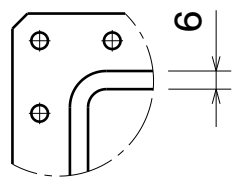
Surépaisseur pour reprise d'usinage



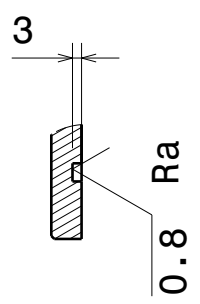
Modification		Author	Date	A
Material:	6060	Ra:	3.2	Project: 064 Advanced-VIRGO
Traitement:	/	Tol:	ISO 2768 mK	Experiment: 10 TableOptique
Qty:	2	Mass:	1.6 Kg	Smarteam SLD: PRT066429
		Dims:	mm	Smarteam DRW: DRW15538
		Scale:	1/5	Date: 2014 March 17
Laboratoire d'Annecy-le-vieux de Physique des Particules BP 110, F-74941 Annecy-Le-Vieux CEDEX		nicolas.allemadou@lapp.in2p3.fr Fax +33 4 50 27 94 95 Ph +33 4 50 09 17 87		
<b>Collier Rallonge Porte</b>		<b>064 10 012</b>		<b>-</b>



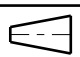
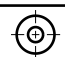

Détail C  
Echelle : 2:5

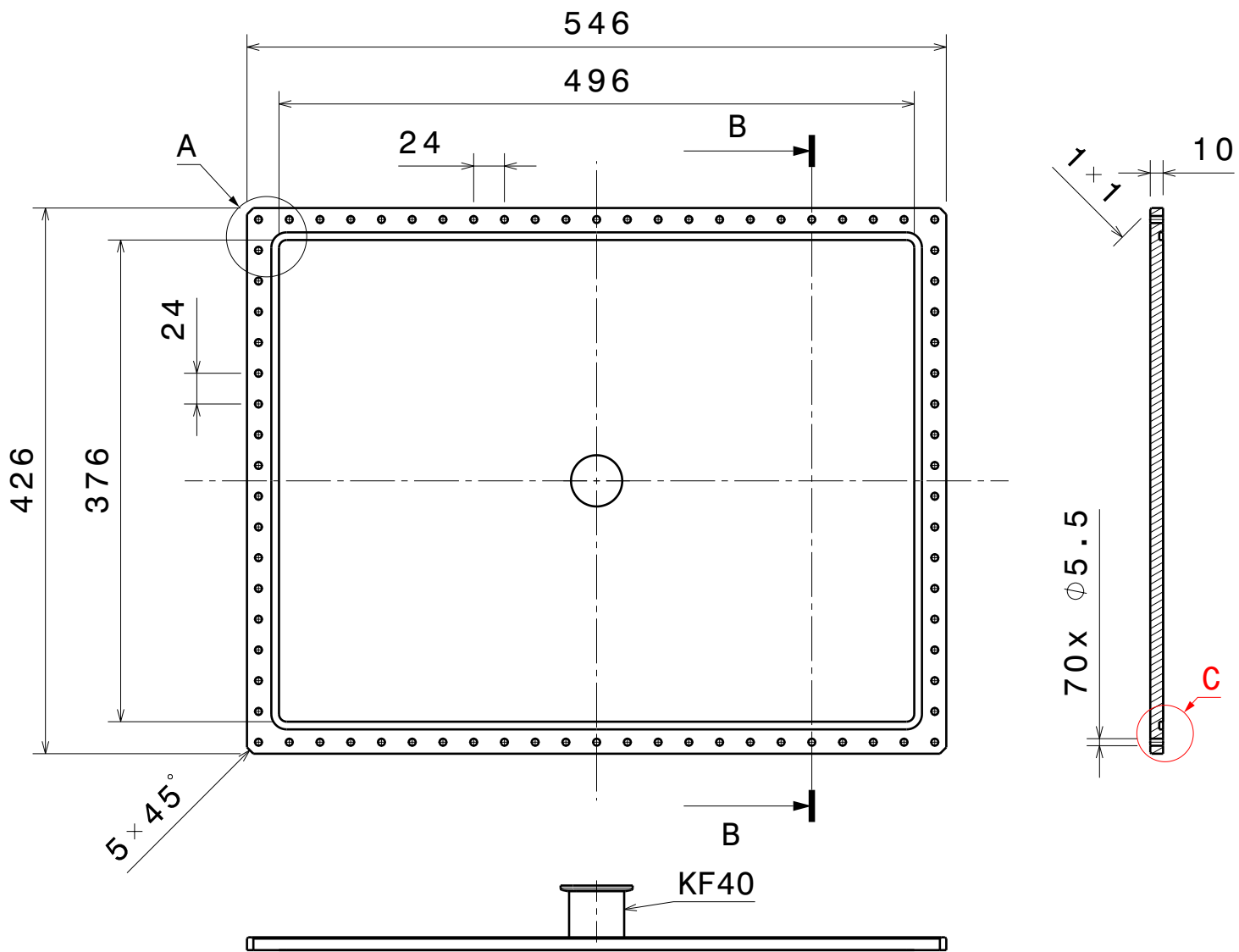


Détail A  
Echelle : 2:5



FranceJoint - IS03601G-55766-533

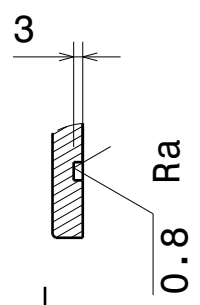
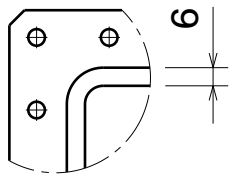
Modification		Author	Date	A
Material:	6060	Ra:	3.2	Project: 064 Advanced-VIRGO
Traitement:	/	Tol:	ISO 2768 mK	Experiment: 10 TableOptique
Qty:	2	Mass:	6.150 Kg	Smarteam SLD: PRT064110
 		Dims:	mm	Smarteam DRW: DRW15195
		Scale:	1/2	Date: 2014 March 17
Laboratoire d'Anncy-le-vieux de Physique des Particules BP 110, F-74941 Anncy-Le-Vieux CEDEX		nicolas.allemadou@lapp.in2p3.fr Fax +33 4 50 27 94 95 Ph +33 4 50 09 17 87		
<b>Detecteur Porte</b>		<b>064 10 020</b>		<b>-</b>



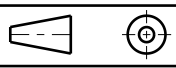

Détail A  
Echelle : 2:5

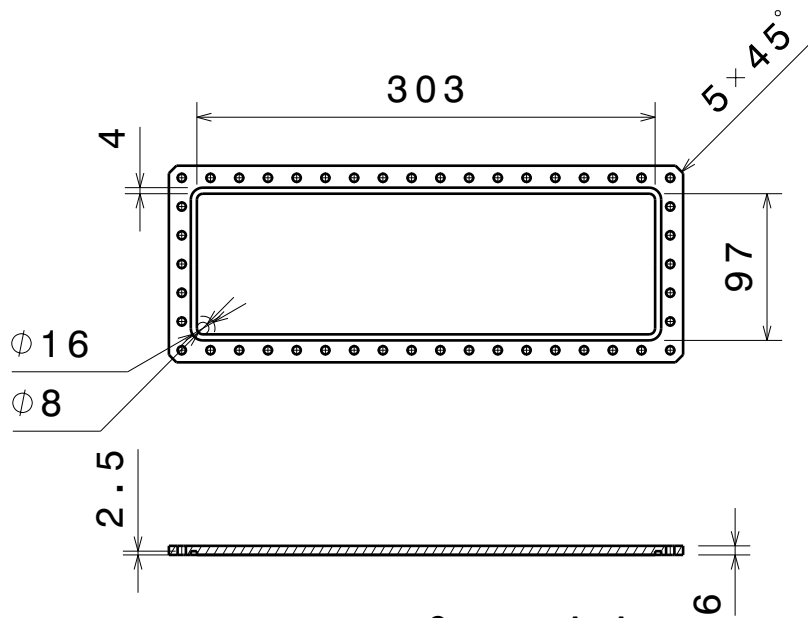
Vue de dessus  
Echelle : 1:5

Détail C  
Echelle : 2:5

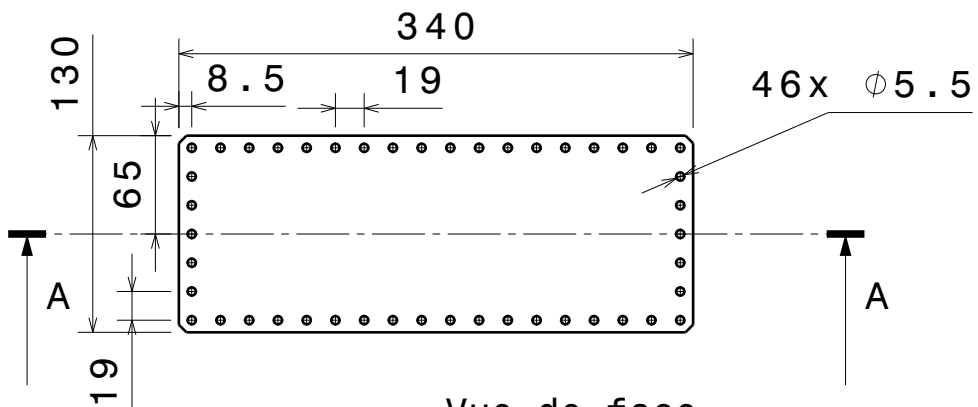


FranceJoint - IS03601G-55766-533

Modification		Author	Date	A
Material: 6060	Ra: 3.2	Project: 064 Advanced-VIRGO		
Traitement: /	Tol: ISO 2768 mK	Experiment: 10 TableOptique		
Qty: 1	Mass: 6.150 Kg	Smarteam SLD: PRT064110		
	Dims: mm	Smarteam DRW: DRW15195		
	Scale: 1/2	Date: 2014 March 17		
Laboratoire d'Anecy-le-vieux de Physique des Particules BP 110, F-74941 Anecy-Le-Vieux CEDEX		nicolas.allemadou@lapp.in2p3.fr Fax +33 4 50 27 94 95 Ph +33 4 50 09 17 87		
Detecteur Porte Pompage		064 10 021		-

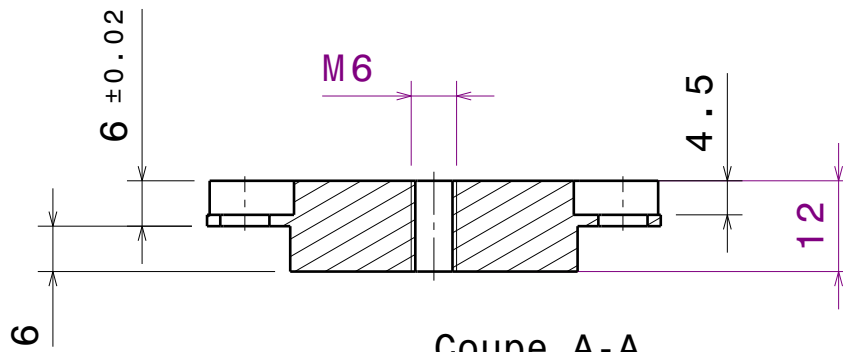


Coupe A-A  
Echelle : 1:5

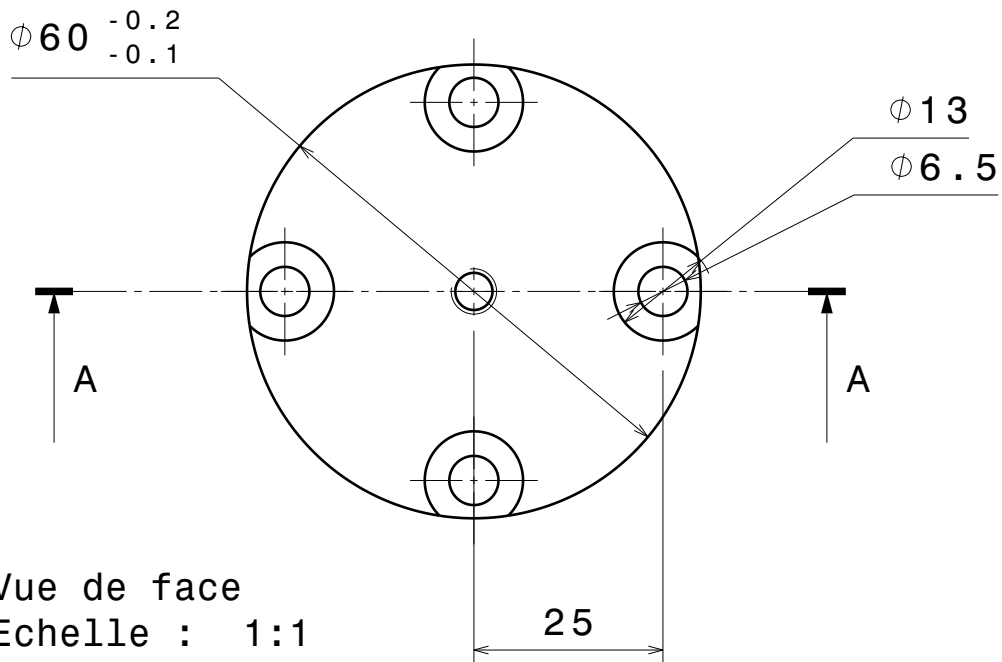


Vue de face  
Echelle : 1:5




Modification		Author	Date	A
Material:	6060	Ra:	3.2	Project: 064 Advanced-VIRGO
Traitement:	/	Tol:	ISO 2768 mK	Experiment: 10 TableOptique
Qty:	4	Mass:	1.3 Kg	Smarteam SLD: PRT069078
		Dims:	mm	Smarteam DRW: DRW15705
		Scale:	1/5	Date: 2014 March 17
Laboratoire d'Annecy-le-vieux de Physique des Particules BP 110, F-74941 Annecy-Le-Vieux CEDEX			nicolas.allemandou@lapp.in2p3.fr Fax +33 4 50 27 94 95 Ph +33 4 50 09 17 87	
<b>Connecteur Plaque Pleine</b>			<b>064 10 026</b>	<b>-</b>



Coupe A-A  
Echelle : 1:1



Vue de face  
Echelle : 1:1

Modification		Author	Date	A
Material:	6060	Ra:	3.2	Project: 064 Advanced-VIRGO
Traitement:	/	Tol:	ISO 2768 mK	Experiment: 10 TableOptique
Qty:	12	Mass:	0.06 Kg	Smarteam SLD: PRT068925
 		Dims:	mm	Smarteam DRW: DRW15770
		Scale:	1/1	Date: 2014 March 17
Laboratoire d'Anecy-le-vieux de Physique des Particules BP 110, F-74941 Anecy-Le-Vieux CEDEX		nicolas.allemandou@lapp.in2p3.fr Fax +33 4 50 27 94 95 Ph +33 4 50 09 17 87		
<b>Bouchon Cable</b>		<b>064 10 041</b>		<b>-</b>